KINETICS AND MECHANISMS OF TITANIUM WIRE OXIDATION

by

Tanmay P. Engineer

A thesis

submitted in partial fulfillment

of the requirements for the degree of

Master of Science in Materials Science and Engineering

Boise State University

December 2012

BOISE STATE UNIVERSITY GRADUATE COLLEGE

DEFENSE COMMITTEE AND FINAL READING APPROVALS

of the thesis submitted by

Tanmay P. Engineer

Thesis Title: Kinetics and Mechanisms of Titanium Wire Oxidation

Date of Final Oral Examination: March 22, 2012

The following individuals read and discussed the thesis submitted by student Tanmay P. Engineer, and they evaluated his presentation and response to questions during the final oral examination. They found that the student passed the final oral examination.

Darryl P. Butt, Ph.D.	Chair, Supervisory Committee
Megan E. Frary, Ph.D.	Member, Supervisory Committee
Michael F. Hurley, Ph.D.	Member, Supervisory Committee
Dmitri A. Tenne, Ph.D.	Member, Supervisory Committee

The final reading approval of the thesis was granted by Darryl P. Butt, Ph.D., Chair of the Supervisory Committee. The thesis was approved for the Graduate College by John R. Pelton, Ph.D., Dean of the Graduate College.

ACKNOWLEDGEMENTS

First of all, I am grateful to my advisor Dr. Darryl Butt for his invaluable guidance during the term of my master's degree. It was his continued faith in me along with persistent support that helped me successfully accomplish this degree. I would like to especially thank Dr. Michael Hurley for his encouragement and his efforts in helping me clarify my research and thesis goals. I would also like to thank the rest of the members of my thesis supervisory committee, Dr. Megan Frary and Dr. Dmitri Tenne, for their constructive feedback on my thesis work. I would also like to thank members of my research group – Brian Jacques, David Thomsen, Adriel Apter, Jeff Huntsinger, Ellen Rabenberg, and Joshua Kane for their help and guidance in collecting data, preparing samples, and providing resources during my research study.

I convey my special thanks to Dr. Rick Ubic, Karthik Chinnathambi, Steve Letournau, and Daniel Leu for their guidance in TEM sample preparation and analysis of TEM results. I would also like to thank Aaron Thuber and the Department of Physics for help in carrying out XPS analysis. I especially thank Jatuporn Burns and Center for Advanced Energy Studies (CAES) for the preparation of TEM samples using FIB, which contributed significantly to my research.

I would like to express my gratitude to Christy Babcock, the International Student Services, and the Department of Materials Science and Engineering at Boise State for

providing a great support system and making my student life in Boise State a very comfortable and enjoyable one.

Finally, without the constant support of my friends, Michael Reff, Atharva Poundarik, and Jatuporn Burns, my brother, Nimit, my father, Piyush, and my mother, Leela, I would have never reached this far in my aspirations.

ABSTRACT

The kinetics and mechanisms of oxidation of titanium wire were assessed using a large test matrix in Ar-20% O_2 at 800 to 1200°C, and N_2-20% O_2 at 1000°C, for 0.5 to 24 hours. The effects of geometry on oxidation were evaluated by investigating the behavior of six high purity Ti wires with diameters varying from 50 to 2000 µm, with an objective of producing hollow TiO_2 tubes.

Oxidation behavior was characterized by measuring oxide thicknesses and morphology by optical microscopy, and the phases were characterized using a combination of SEM and TEM. The kinetics was evaluated using a shrinking core model derived for cylindrical geometry. Activation energies for oxidation were obtained from fits of experimental data to the model and calculated values generally agreed well with values reported in the literature for bulk Ti.

It is suggested that oxygen dissolution in the residual Ti is the overall rate limiting mechanism between 800-1200°C at shorter oxidation durations. At longer durations, the oxide is multi-layered, susceptible to spallation, and consequently the mechanism is complex. It is demonstrated that due to the fast outward diffusion of Ti, the oxide grows outward, resulting in the separation of the oxide from the oxygen-saturated metal core, in some cases leading to the formation of hollow TiO_2 tubes.

TABLE OF CONTENTS

LIST OF FIGURES

LIST OF TABLES

LIST OF SYMBOLS

α	fraction of the reacted volume of the solid
E_A	activation energy
k_P	parabolic rate constant of the reaction
k_L	linear rate constant of the reaction
k_C	cubic rate constant of the reaction
L	length of the wire
R	initial radius of the solid
r	radius of the residual solid after reaction
t	oxidation time
T	temperature in degree Kelvin
x	oxide thickness in microns

CHAPTER ONE: INTRODUCTION

1.1 Motivation for Research

Titanium and its alloys are well known for their widespread applications in many diverse fields including, spacecraft, submarines, automobiles, sports equipment, and implant materials. They are considered technically and mechanically advanced and cost-effective substitutes in many structural components mainly due to their relatively high strength-to-weight ratio, exceptional aqueous corrosion resistance, creep and fatigue resistance, good ductility, hot formability, and toughness. Titanium exhibits excellent mechanical properties and oxidation resistance to approximately 600°C, above which it oxidizes rapidly and is prone to dissolve gases like oxygen, nitrogen, and hydrogen [1]. Although, oxidation is generally undesirable, it is possible to use oxidation as a means for fabricating titanium oxide-based devices or components for possible applications as photo catalysts, dye-sensitized solar cells, gas sensors, and others [2]. TiO_2 coated roof panels and bricks also help in absorbing nitrogen oxide (NO) and keeping the environment clean [3]. Hence, a detailed study of the titanium oxidation process is of great significance.

Detailed investigations on high temperature oxidation of titanium have been conducted in the past [4-26]. A review of these investigations suggests that titanium oxidation involves varying oxidation mechanisms and oxide-scale morphology depending on the temperature and duration of oxidation; hence, the mechanism of oxidation is

complex. This complication is also attributed to the competitive process of the formation of a multi-layered oxide scale and simultaneous excessive dissolution of oxygen in the base metal. Depending on the oxygen gradient at the surface and scale-metal interface, there is a possibility of forming various oxides of titanium within the scale. Furthermore, pure titanium undergoes an allotropic transformation from the hexagonal closed packed (HCP) α phase to the body centered cubic (BCC) β phase at 882°C. The α-phase may be stabilized by oxygen dissolved in the metal. This further complicates the mechanism of oxidation, as at higher temperatures oxygen dissolution not only involves dissolution in the β phase but also the use of oxygen in the growth of the α-phase.

Titanium and its alloys have been used for structural applications in various shapes like sheet, bar, plate, tubing, disks, gears, engine cases, blades, and hydraulic cylinders [1]. However, a review of the literature reveals that except a very few [21, 22, 27, 28], most of the titanium oxidation studies have been focused on planar geometry only. Hence, detailed investigations of titanium oxidation in other geometries and their comparison with that in planar geometry are required. Moreover, following an observation of the formation of titanium oxide hollow tubes upon oxidation of fine titanium wires by Butt [29] as shown in Figure 1, the present study was focused on investigating the kinetics and mechanism of the oxidation of titanium wires and studying the formation of oxide hollow tubes.

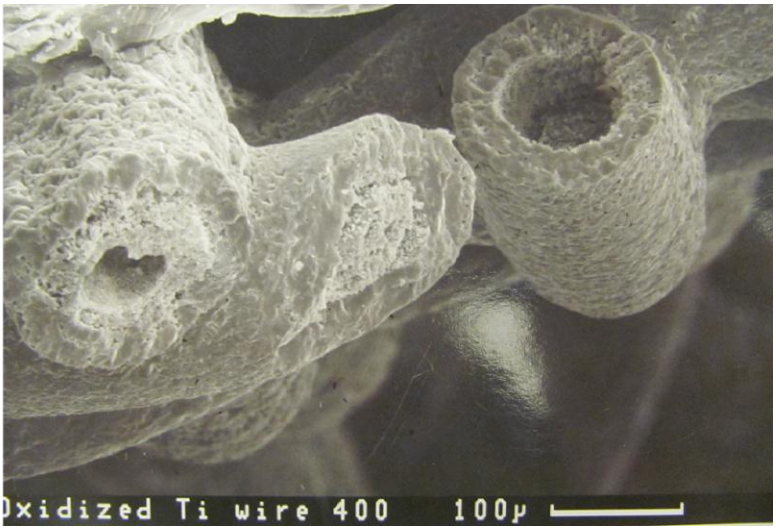

Figure 1: A SEM micrograph of an oxidized titanium wire showing formation of a TiO_2 hollow tube [29].

1.2 Objectives

The objectives of this research were to experimentally characterize the oxidation kinetics of Ti wire and develop a model that accounts for geometry in order to determine pertinent kinetics parameters including parabolic rate constants and activation energies for oxidation. In addition, an objective was to identify optimal conditions of oxidation of Ti wire for producing hollow titanium oxide micro-tubes through an understanding of these kinetics data, for potential applications as photo-catalysts or solar cell materials.

CHAPTER TWO: LITERATURE SURVEY

2.1 The Titanium-Oxygen Phase Diagram

To better understand high temperature oxidation of titanium, Ti-O phase diagrams as shown in the Figure 2 and Figure 3 were considered.

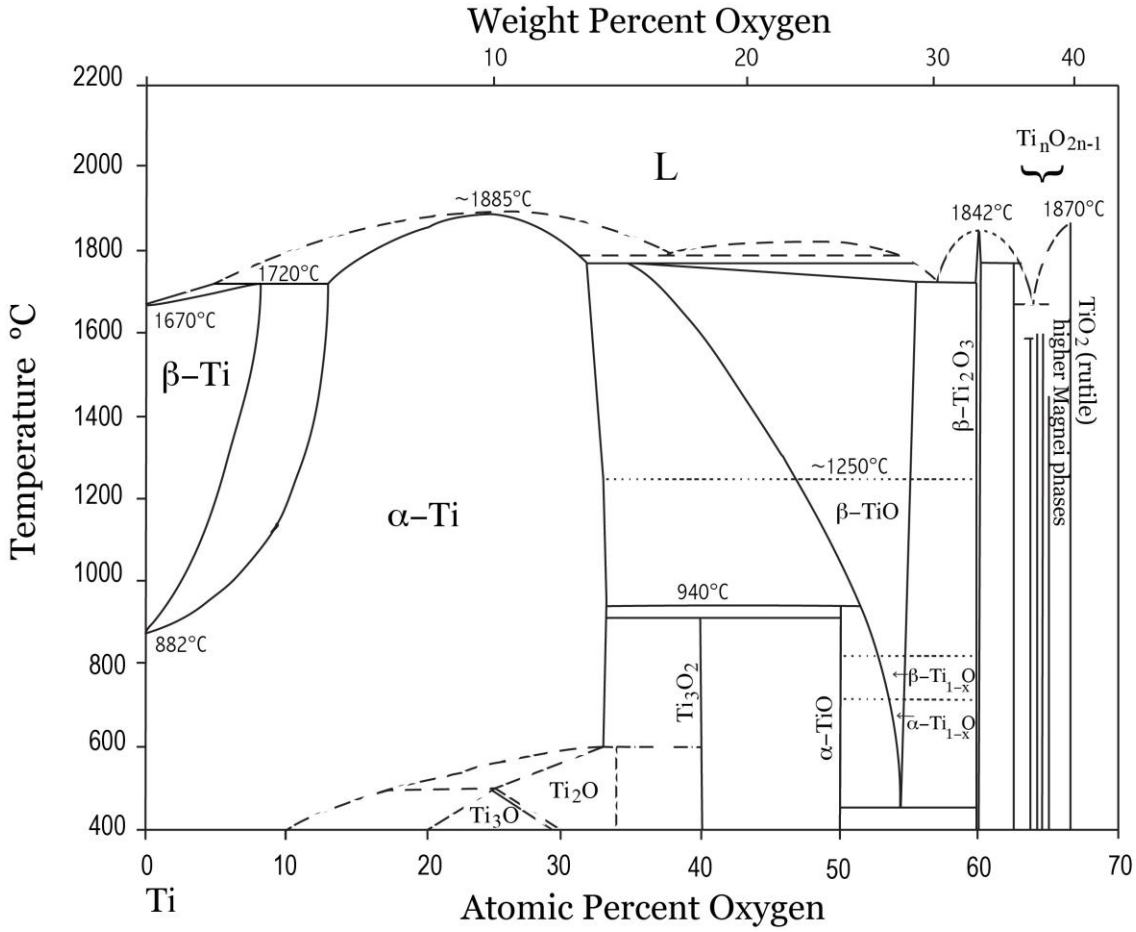

Figure 2: A re-drawn Ti-O phase diagram based on Murray and Wriedt [30]. The diagram shows α-β titanium phase transformation at 882°C. It also shows that oxygen acts as a α phase stabilizer.

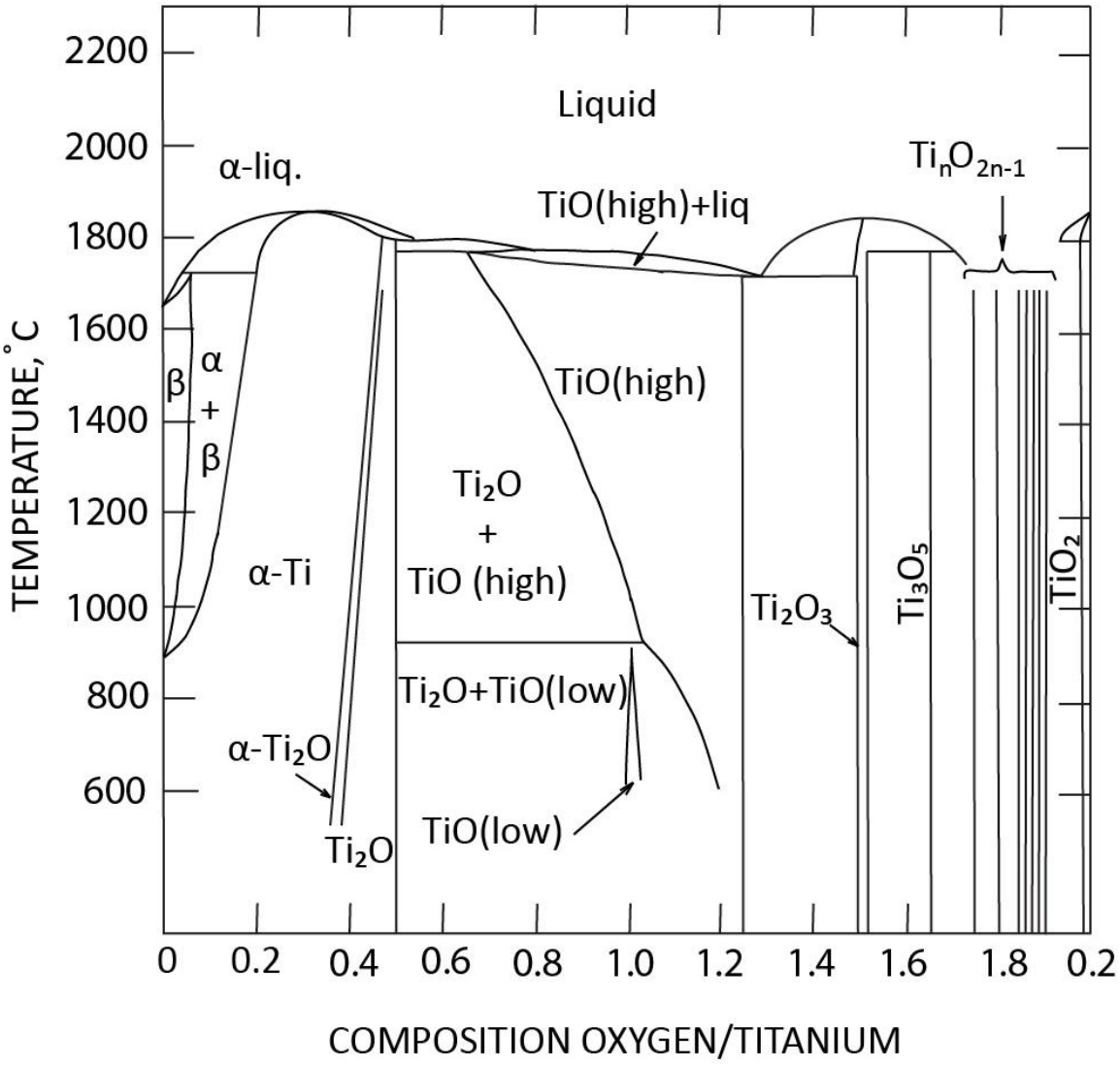

Figure 3: A re-drawn Ti-O phase diagram by Wahlbeck and Gilles [31]. The phase diagram shows the presence of a distinct Ti_2O phase boundary in contrast to the Ti-O phase diagram by Murray and Wriedt.

As can be observed from Figure 2, below the α-β transition temperature at 882°C, oxygen dissolves in the α phase to approximately 33 atomic percent. Above 882°C, as oxygen is an α-phase stabilizer, oxygen initially dissolves in β-phase and eventually helps in transforming the β-phase to the α-phase. The solubility of oxygen in the β-phase

increases slightly with temperature to a maximum of approximately 8 atomic weight percent oxygen at 1720°C.

As far as the kinetics of oxygen dissolution is concerned (and considering Figure 3), according to Hurlen, the oxygen dissolution in the α-phase is of negligible importance below 500°C, while in a temperature range of 600 to 700°C oxygen dissolves readily up to 14-15 atomic percent [20]. Kofstad suggested that the oxygen solubility further increases at higher temperatures, especially above 900°C, where titanium exists in its β form [4]. This is because the oxygen diffusion in the β-phase has lower activation energy and is faster than that in the α-phase. However, the oxygen solubility in the β-phase is smaller than that in the α-phase, and hence, a major fraction of the oxygen is consumed in the formation of the α-phase. The difference in the solubility of oxygen and activation energy of oxygen dissolution in the α-phase and the β-phase lies in the difference in the crystal structures of the two phases. α-Ti has a hexagonal crystal structure while β-Ti has a body centered cubic crystal structure.

As can be inferred from the Ti-O phase diagrams, TiO_2 (rutile) is the most oxygen-rich form of stable oxide that titanium forms with oxygen. Even though it is thermodynamically favorable to form different layers of oxides of titanium, namely Ti_2O, TiO, Ti_2O_3, Ti_3O_5, and TiO_2 in oxygen at near atmospheric pressure, only the rutile modification of TiO_2 has been found below 1000°C [5]. However, there is evidence of the formation of the lower oxides of titanium at reduced oxygen pressures and higher temperatures.

2.2 Kinetics and Mechanisms of High Temperature Oxidation of Titanium

As pointed out earlier, numerous researchers (including Kofstad [4], and Kofstad *et al.*[5, 6], Jenkins [7, 8], Stringer [10-12], Davies and Birchenall [13], Morton and Baldwin [14], Gulbransen and Andrew [26], and many more) have investigated the high temperature oxidation of titanium. These investigations assessed the effects of oxidation temperature, time, oxidizing environment, and oxide scale morphology on the oxidation kinetics and mechanisms. The calculation of reaction rates and activation energy of oxidation were also done by numerous investigators. These studies are explained in detail in the following sections.

2.2.1 Effect of Oxidation Temperature and Time

According to previous investigations, oxidation in titanium in different temperature ranges occurred under different rate laws. Kofstad *et al.* [6] proposed that below 300°C, oxidation followed a logarithmic rate law. Similar studies by Smith [32], and Alexander and Pidgeon [33] in the temperature range of 25 to 400°C also suggested that the oxidation followed a logarithmic rate law. Investigations by Hurlen [20] also suggested that the oxidation followed a logarithmic rate law up to 500°C. According to Kofstad *et al.*[6], at a temperature below 600°C, the oxidation followed a cubic rate law.

In the temperature range 600-850°C, many researchers concur that the oxidation process proceeds by a parabolic rate law, which however, upon prolonged oxidation exhibits a pseudo-linear behavior [6, 7, 14, 20, 26]. Such parabolic oxidation involves simultaneous dissolution of oxygen and oxide scale formation, both occurring with parabolic kinetics, individually. With the exception of Gulbransen and Andrew [26] and

Hurlen [20], most researchers believed that the parabolic oxidation resulted from the diffusion of oxygen ions through the oxygen ion vacancies present in the oxide layer.

Above approximately 850°C, oxidation tends to obey a linear rate law, after an initial parabolic law. It was a general observation that the higher the temperature of oxidation, the shorter was the duration in which the linear rate law was attained [4, 5]. There are relatively two different observations on how the linear oxidation proceeds in this temperature range:

1. When oxygen dissolution in the metal results in a composition of $TiO_{0.35}$ in the exterior of the metal, heavy oxidation starts to occur, resulting in pseudo-linear oxidation [5]. It has been proposed that when the metal outer layer reaches such composition, cracking of this metal layer occurs due to the growth of stresses from the expansion of the lattice by oxygen dissolution. Thus, the detached layer, due to a sudden high availability of oxygen, undergoes rapid oxidation [4, 5, 10, 12].
2. However, Lopes Gomes and Huntz [17], Bertrand *et al.* [19], and Stringer [12] believed that the linear behavior is actually a series of parabolic steps resulting from successive parabolic oxidation of new oxide layers formed upon a detachment of the previous oxide layers. Oxidation in such a fashion resulted in an oxide scale with multiple layers with approximately equal thickness.

Upon prolonged oxidation above 850°C, the linear oxidation is followed by a period of second parabolic oxidation. According to Stringer [10], this second parabolic rate law is associated with rate limiting diffusion of the gas through the porous oxide scale. On the other hand, Kofstad *et al.* [5] believed that this decreased oxidation is associated with the densification of the outer oxide layer due to sintering accompanied

with grain growth. Different reaction kinetics observed in relation to the oxidation temperature and time during titanium oxidation can be summarized as follows in Figure 4.

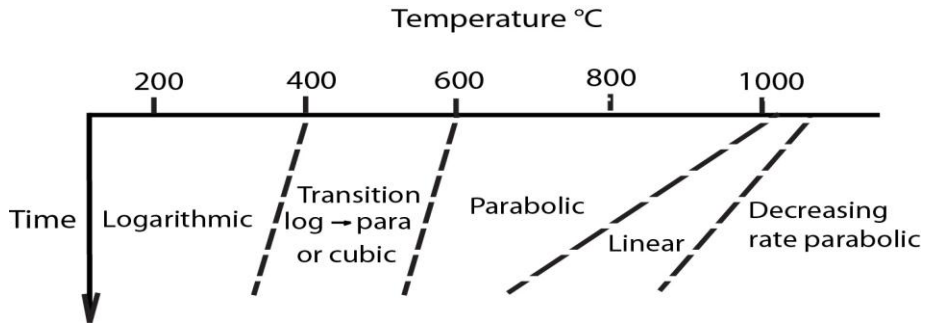

Figure 4: Schematic diagram based on Kofstad [34] representing different rate laws observed during oxidation of titanium.

The complications in the oxidation mechanism of titanium above 850°C are also due to the α-β titanium transition temperature at 882°C. As mentioned earlier, in this temperature range, oxygen is consumed not only via dissolution in the β-phase but also in the growth of the α-phase. However, α-Ti is the initial phase present for oxidation at higher temperatures because oxygen being an α-stabilizer transforms most of β-Ti in α-Ti within very short duration of oxidation.

2.2.2 Measurements of the Reaction Kinetics

The knowledge of reaction rates and kinetics can provide valuable information about the reaction mechanism and the rate-limiting step of the overall reaction. Rate measurements also serve as a basis for a numerical description of the reaction behavior that is invaluable for comparison with theoretical models [35]. The extent of the reaction can be measured by measuring the following:

1. The amount of metal consumed, which is measured by either observing the weight loss of the specimen or the residual metal thickness.
2. The amount of oxygen consumed, which is measured by observing either the weight gain or the amount of oxygen used from a specific volume.
3. The amount of oxide produced by measuring either the weight of the oxide formed or the oxide thickness.

In order to deduce oxidation kinetics, the extent of oxidation is measured as a function of time and temperature [36]. Studies of reaction rates or kinetics of titanium oxidation have been carried out by a combination of the following methods:

1. Thermo-gravimetric analysis: This method involves measuring the weight change of the titanium specimen continuously as it undergoes an oxidation reaction.
2. Volumetric and manometric methods: This method involves measuring the pressure drop in the system due to oxygen consumption or measuring the volume consumed.
3. Oxide thickness measurements: Some researchers measured the thickness of the oxide formed after the oxidation reaction for a specific span of time [21, 22, 28]. This method, even though it requires multiple samples, is quite useful to obtain kinetics data as one can assess the morphology of the oxide scale in much detail.

The rate constants usually increase as the temperature is raised and can be related to the Arrhenius behavior as represented in Equation 1 below.

$$\ln k_P = \ln \mathrm{A} - E_A/\mathrm{R}T \quad (1)$$

A plot of ln kP versus 1/T gives a straight line with the slope as E_A/R, Y-intercept as A called the pre-exponential factor E_A, the activation energy, and R, the gas constant.

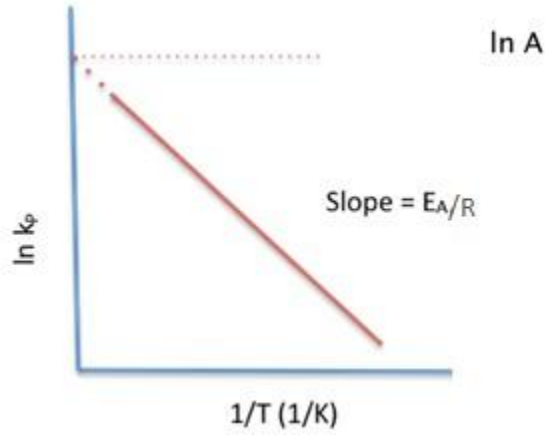

Figure 5: A schematic representation of a general Arrhenius plot.

2.2.3 Oxide Scale Morphology

Oxide scale morphology is usually observed using either a scanning electron microscope (SEM) or an optical microscope. The stable oxides of titanium include Ti_2O, TiO, Ti_2O_3, Ti_3O_5, Ti_nO_{2n-1} ($4<n<38$), and TiO_2. It is thermodynamically feasible that a titanium oxide scale may consist of a sequence of layers of the different oxides of titanium [34]. The oxide scale morphology was usually found to change with the change in oxidation kinetics.

Below 400°C, the oxidation kinetics was found to be logarithmic such that the rate of oxide growth eventually leads to a constant oxide thickness with time and the oxide film was metallic grey in appearance [32]. The oxide scale during cubic kinetics in the temperature range 400-600°C appears similar to the one during logarithmic (i.e., metallic grey), the only difference being that the oxygen dissolution in titanium tends to become more dominant with an increase in the temperature of oxidation. During

parabolic oxidation from 600-850°C, the oxide scale is found to be adherent, and dark grey or blue in appearance [6, 14]. Morton and Baldwin [14] proposed that upon prolonged oxidation below 850°C, the scaling layer is loosely attached to titanium and forms a layer of TiO between the metal and the TiO_2 layer. Upon prolonged oxidation in this temperature range, the adherent oxide scale cracks and splits from the metal surface and further reacts with oxygen becoming a stoichiometric scale, which is light grey or white in appearance [10].

Above 850°C, where the oxidation kinetics is essentially linear, the oxide scale is porous and consists of fine oxide layers of equal thickness [6, 10]. Furthermore, extended oxidation in the temperature range from 875°C to 1050°C results in the formation of a thin layer of Ti_2O_3 between the TiO and TiO_2 layers [14]. There are also findings of the formation of a compact outer oxide layer due to sintering and grain growth, along with a porous inner oxide layer, that is either white or light yellow in appearance [5].

2.2.4 Effects of Oxidizing Medium

Most of the titanium oxidation studies have been conducted in pure oxygen [4-13, 19, 20, 32]. Only a few were carried out in air [14, 18, 24, 37], mixed nitrogen-oxygen, argon-oxygen atmosphere [23, 25, 38], or in water vapor [39].

Morton and Baldwin's [14] oxidation studies in air from 850 to 1000°C showed that the scaling initially followed a slow parabolic rate constant but, after a certain time, a much faster second parabolic rate law took over. This transition to a more rapid regime of kinetics, rather than linear kinetics (as observed in pure oxygen), was caused by the nucleation and growth of a new blue colored rutile scale having a much higher electrical conductivity.

In contrast to the above observations, oxidation studies by Chen and Rosa [40] on a Ti-4.37 wt.% Ta alloy in both pure oxygen and air revealed a relatively decreased oxidation rate in air than in pure oxygen. Similar studies by Hanrahan and Butt [23] on the Ti-5 wt.% Ta alloy demonstrated that oxidation rates in air and N_2-20% O_2 were significantly lower than those in Ar-20% O_2. They proposed that this decreased oxidation rate was due to the formation of a nitride layer (TiN as determined using TEM), which acts as an oxygen diffusion barrier, thereby reducing the extent of oxygen dissolution in the substrate. Gobel *et al.* [38] proposed that upon oxidation at 800°C for 150 hours in nitrogen containing atmospheres, the amount of dissolved nitrogen in pure titanium is significantly lower than the amount of oxygen and causes only a slight decrease in the oxidation rate with respect to that in pure oxygen. As in the case of the oxidation of titanium in water vapor, Perez [39] found the oxidation rate to be slower than that in pure oxygen at 900°C.

The effect of varying oxygen pressure was studied by a few investigators like Kofstad [4], Gulbransen and Andrew [26], and Hurlen [20]. On the basis of their studies in the temperature range 700-1000°C, Kofstad concluded that the titanium oxidation is dependent on the oxygen pressure under the linear rate law (e.g., at 900 to 1000°C), whereas it is independent of the oxygen pressure under the parabolic rate law (e.g., at 700 to 800°C). They were also able to prove that the duration of the cubic rate law decreases with increasing oxygen content and almost disappears for highly oxygen-saturated titanium. Observations by Hurlen, and Gulbrensen and Andrew also concurred that the parabolic oxidation is completely independent of changes in oxygen pressure.

2.2.5 Effects of Geometry

Titanium oxidation, as we understand, has quite a complicated mechanism. Most of the titanium oxidation studies were done on planar geometry only. However, titanium is used commercially in various shapes and sizes. Thus, understanding its oxidation behavior in multiple dimensions, and the effects of specific shapes in influencing its oxidation mechanism is of great significance.

There have been only a few studies that have focused on oxidation mechanism of metals in different shapes. Some of the pioneering work on high temperature oxidation in non-planar geometries was performed by Jander [41] and Carter [42]. More recently, a general kinetic relationship for the oxidation of cylindrical fiber was derived by Zhu *et al.* [28] and Jiang *et al.* [43].

Effects of non-planar geometries and volumetric oxidation during the oxidation of titanium were studied in detail by Entchev *et al.* [21], and Imbrie and Lagoudas [22]. They carried out oxidation studies in titanium in solid and hollow cylinders and internal and external wedges, and compared the oxidation of these geometries with planar oxidation. Their study was conducted at 700°C, during which titanium exhibits parabolic oxidation. They also deduced kinetic relationships for the oxidation of titanium in planar, cylindrical, and spherical geometry. Their work showed that the oxidation kinetics in solid cylindrical and external wedge-shaped geometries is faster than that in planar geometry; however, hollow cylindrical and internal wedge-shaped specimens showed a slower oxidation rate.

Using an inelastic approach and the perturbation analysis, a kinetics study on cylindrical and spherical geometries was carried out by Oh [27]. However, the studies

focusing on the effects of geometry on titanium oxidation are either limited to a single oxidation temperature and oxidizing medium (for example, in the studies by Imbrie and Lagoudas) or are related to mere theoretical derivations (for example, in the studies by Oh). Abundant experimental data related to the oxidation of titanium in non-planar geometries in various temperature ranges and oxidizing mediums is still not available.

2.3 Summary of the Background of High Temperature Oxidation of Titanium

A review of high temperature oxidation studies of titanium suggests that the mechanism of titanium oxidation is quite complicated due to changing reaction kinetics and competing oxidation reactions. Numerous researchers have conducted extensive studies and investigated different conditions of high temperature oxidation of titanium in planar geometry. However, studies of the oxidation mechanism of titanium and morphological evolution of oxide scale under different oxidizing conditions like temperature, time, and oxidizing mediums for non-planar geometries are required.

The present work was focused on oxidation kinetics and morphological evolution investigations on titanium wires (non-planar geometry) in the temperature range of 800-1200°C with oxidation time varying from 0.5 to 24 hours. To assess the effects of size, six different diameter titanium wires ranging from 50 to 2000 microns were employed for the oxidation studies. Oxidation was carried out in an argon-20% oxygen (Ar-20% O_2)/ nitrogen-20% oxygen (N_2-20% O_2) gas mixture to compare the oxidation kinetics of titanium wires in these two mediums.

CHAPTER THREE: EXPERIMENTAL METHODS

3.1 Oxide Thickness and Metal Core Diameter Measurements

3.1.1 Sample Oxidation Procedure

Varying the following four parameters, an extensive observation of high temperature oxidation of titanium wire was carried out:

1. titanium wire diameter,
2. oxidizing environment,
3. temperature of oxidation, and
4. time span of oxidation.

To carry out a single oxidation profile, pure titanium wires (99.99%, Alfa Aesar, Ward Hill, MA, USA) of six different diameters (50, 127, 250, 500, 1000, and 2000 μm) were used. To carry out oxidation in a controlled atmosphere, a high temperature tube furnace (CM furnace, Bloomsburg, NY, USA) was used. The wires were cut to the lengths slightly greater than the width of an alumina boat over which they were suspended as shown in Figure 6 below.

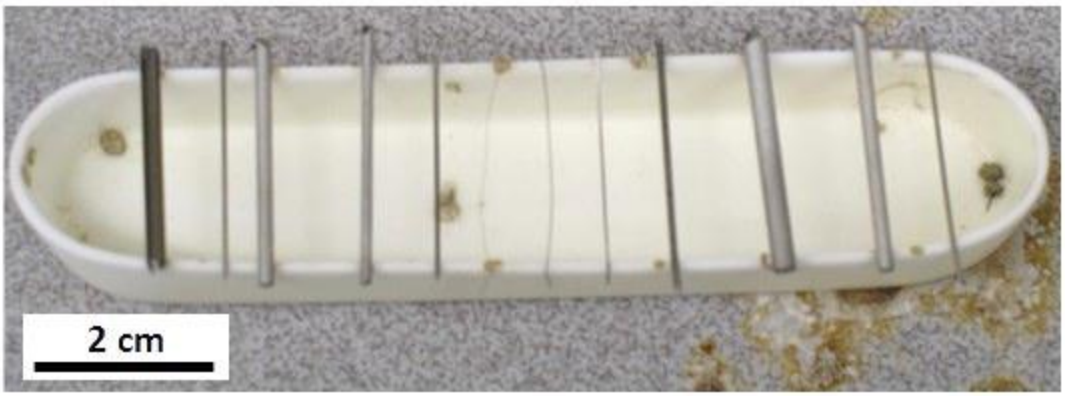

Figure 6: An optical image representing the placement of the titanium wires of different diameters over the alumina boat for carrying out oxidation in the high temperature tube furnace.

The alumina boat containing the wires was placed in the center of the hot zone of the tube furnace, while at room temperature. The ends of the furnace tube were sealed using vacuum sealing flanges to allow for an atmosphere control.

The samples were heated at the ramp rate of 250˚C per hour to the required oxidation temperature. Ultra high purity argon gas was allowed to flow in the furnace during the ramping stages while the furnace atmosphere was switched to Ar-20% O_2/N_2-20% O_2 gas mixture during the dwell stage of the heating profile to ensure isothermal oxidation. The argon gas was purified to parts per trillion of oxygen content using the Oxygen Purifier (Restek, Bellefonte, PA) and the purity was recorded using the Oxygen Analyzer (Ntron, Miramar, FL), each wire connected in conjunction with the argon gas line. A simple schematic diagram that represents one of the oxidation profiles used in present work is shown in Figure 7.

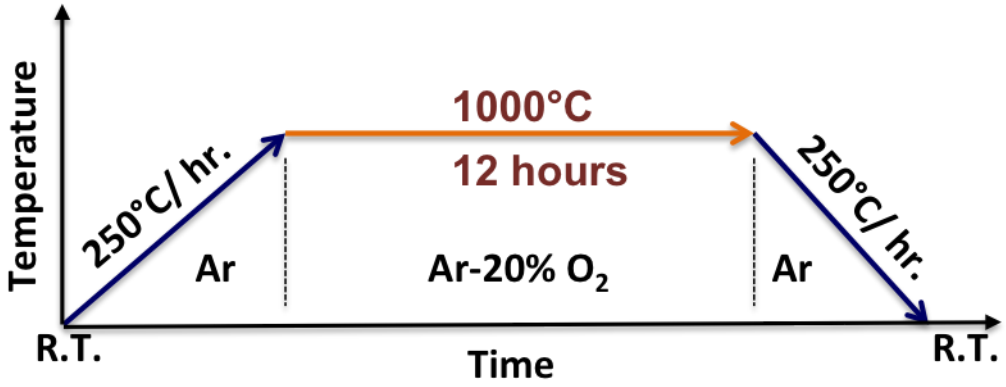

Figure 7: A schematic representing a typical heat treatment profile used in the present work.

3.1.2 Sample Preparation Procedure

Numerous samples were prepared by following the above procedure to have a thorough investigation of the oxidation behavior of titanium wires at high temperature. A sample oxidation matrix that gives an account of all the samples prepared in the temperature range 800-1200˚C is shown in Table 1.

Table 1: A Comprehensive Sample Preparation Matrix. The spots marked with 'x' represent oxidation in Ar-20% O_2 while the ones marked with 'o' represents oxidation in N_2-20% O_2.

Time (hrs.)/ Temp. (°C)	0.5	1	2	3	4	6	8	10	12	16	20	24
800					x		x		x	x		
900					x		x			x		
1000	x	x	x	x	xo	x	xo	x	xo	xo	x	xo
1100										x		x
1200	x	x	x	x	x		x		x	xo		x

Apart from using six different diameters of Ti wires, further statistical data were obtained using 2 approaches:

- Different diameter wires were oxidized for multiple times with identical parameters like similar oxidation time, temperature, and oxidizing environment to get multiple cross-sections.
- A number of similar diameter wires were oxidized together to obtain multiple cross-sections.

The oxidized samples so obtained were mounted in a two component epoxy (Leco, St. Joseph, MI, USA) and polished to 0.5 µm along their circular cross-sections using the variable speed grinder-polisher (Ecomet 300, Buehler), the silicon carbide polishing discs, and the diamond paste (Leco, St. Joseph, MI, USA).

3.1.3 Sample Cross-Section Imaging

Once the samples were polished down to 0.5 µm, magnified optical images of the sample were obtained using an optical microscope (Zeiss-Axiovert 200, Thornwood, USA). Basically, three kinds of imaging details were obtained using this tool. The information obtained from them is as follows:

- Bright field imaging:

  Bright field imaging was used to examine, at higher magnification, either the surface roughness of as received samples or to examine the morphology of metal-oxide interface, outer oxide, metal core, intermediate porous oxides, and other distinguishable phases appearing in bright field. The measurements of the residual metal core diameter, and the thickness of various oxides and the intermediate phases

observed in the oxidized samples were obtained primarily from the bright field images.

- Dark field imaging:

  This mode of optical imaging helped to distinguish between different phases present in the oxidized samples with respect to density or porosity of the phases. It was used to obtain a detailed analysis of features in oxides like the appearance of lamellae, cracks, unusual porosity, etc.

- Diffraction Interference Contrast (DIC) Imaging:

  It is an optical illumination technique, which was used to enhance the contrast in unstained, transparent samples. It was used to effectively distinguish phases that are present in minute quantities in the oxidized samples with the help of color contrast. It was useful to examine finer details in samples that were not obtained from bright field or dark field images like in distinguishing phases using difference in grain size or grain orientation, etc. This kind of imaging proved to be extremely helpful in observing and correlating progressive dissolution of oxygen in β-Ti metal core and its conversion to α-Ti with respect to an increase in oxidation time.

3.1.4 Procedure for the Oxide Thickness and Core Radius Measurements

The oxide thickness and core diameter values for wires of all sizes were measured from the bright field images obtained using the Zeiss optical microscope. Simple analysis software called ImageJ (by the National Institute of Health) was used for carrying out measurements. 6-10 readings of oxide thickness and metal core diameter were taken and the average of these six values was considered for plotting relevant graphs.

In some samples, multiple layers of different oxides were clearly visible and thus their thicknesses were individually measured and recorded. In certain samples, the core was completely consumed during oxidation and only an outer layer of oxide was observed. Such samples had small fragments of the oxide in the core. In such cases, the porous core was still measured separately and recorded.

All the data obtained from the measurements were used in deducing and analyzing the relation between oxide thickness or core diameter and parameters including oxidation time, temperature, wire diameter, and environment on oxidation behavior. The oxide thickness or core diameter versus oxidation time data was used in gathering kinetics data and comparing it with the data available in the literature. The oxide thickness or core diameter data can also be used to fit it in a fundamental kinetics model and deducing conclusions regarding probable mechanism of Ti wire oxidation.

3.2 Transmission Electron Microscopy (TEM)

Titanium on oxidation at high temperature forms different layers of oxides including TiO with the rock salt crystal structure, Ti_2O_3 with the rhombohedral rhombahedral structure, TiO_2 (rutile) with tetragonal structure, and other non-stoichiometric oxide phases (Ti_nO_{2n-1}). Also, pure titanium undergoes transition from the hexagonal α-Ti to the BCC β-Ti at 882˚C. TEM can help in analyzing these distinct phases present in minute quantities in the oxidized titanium wires.

The steps used to prepare most samples for TEM analysis are described in Figure 8. The process includes the following basic steps:

1. Mounting the oxidized samples in 3 mm diameter copper tube,

2. Sectioning the copper mounts along their circular cross-sections to obtain 1.5 mm thick discs,
3. Polishing the discs to 6.5 µm finish on both sides using a disc grinder until they are 25-30 µm thick,
4. And finally, polishing the discs using the precision ion polishing system to make them suitable for observation in TEM.

In addition, the FAE-Quanta 3D FEG focused ion beam (FIB) available at Center for Advanced Energy Studies (CAES), Idaho Falls was used to prepare some other TEM samples.

The TEM used to analyze this sample is JEOL JEM-2100 available at the Boise State Center for Materials Characterization (BSCMC). It was operated at 200kV and is also coupled with capabilities like EDS, Scanning Transmission electron microscopy (STEM), and a Gatan Orius SC 1000 CCD camera.

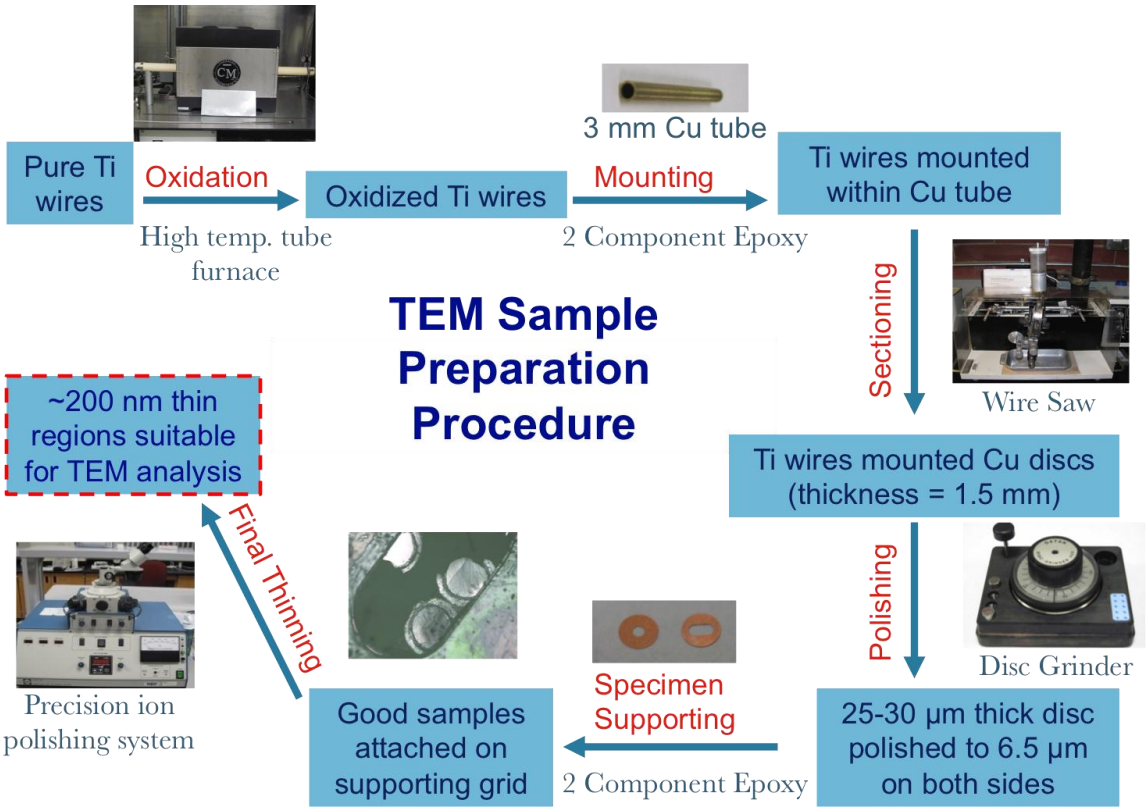

Figure 8: The sample preparation procedure for obtaining desirable TEM samples for the present study.

CHAPTER FOUR: RESULTS

4.1 Oxidation Kinetics of Titanium Wire

The knowledge of reaction rates and kinetics provide valuable information about the reaction mechanism and the rate-limiting step of the overall reaction [35]. In the present work, reaction rates were obtained by measuring both the oxide thickness and the remaining core diameter in the oxidized samples. Since numerous samples showed the presence of a multi-layered oxide scale having regions with varying densities, the oxide thickness measurements were not as reliable as residual core diameter measurements for performing kinetics analysis. Hence, the residual core diameter measurements are reported in this section while the oxide thickness measurements are instead provided in Appendix A.

The core diameter vs. oxidation time data for oxidation at 800°C, 1000°C, and 1200°C are presented in Figure 9, 10, and 11, respectively. Each data point in the plot for 800°C and 1200°C represents an average value of 6-10 measurements of residual core diameter over a single cross-section of the specific diameter wire concerned. The collection of data was much more extensive at 1000°C as the measurements were carried out over 4-6 different cross-sections (instead of a single cross-section as in the case of 800°C and 1200°C). Each error bar in the plots represents the highest and the lowest value of the core diameter measured. The data points for 50 and 127 μm diameter wires are not presented in the plot for oxidation at 1000 and 1200 ºC because they were completely oxidized in less than 2 hours of oxidation.

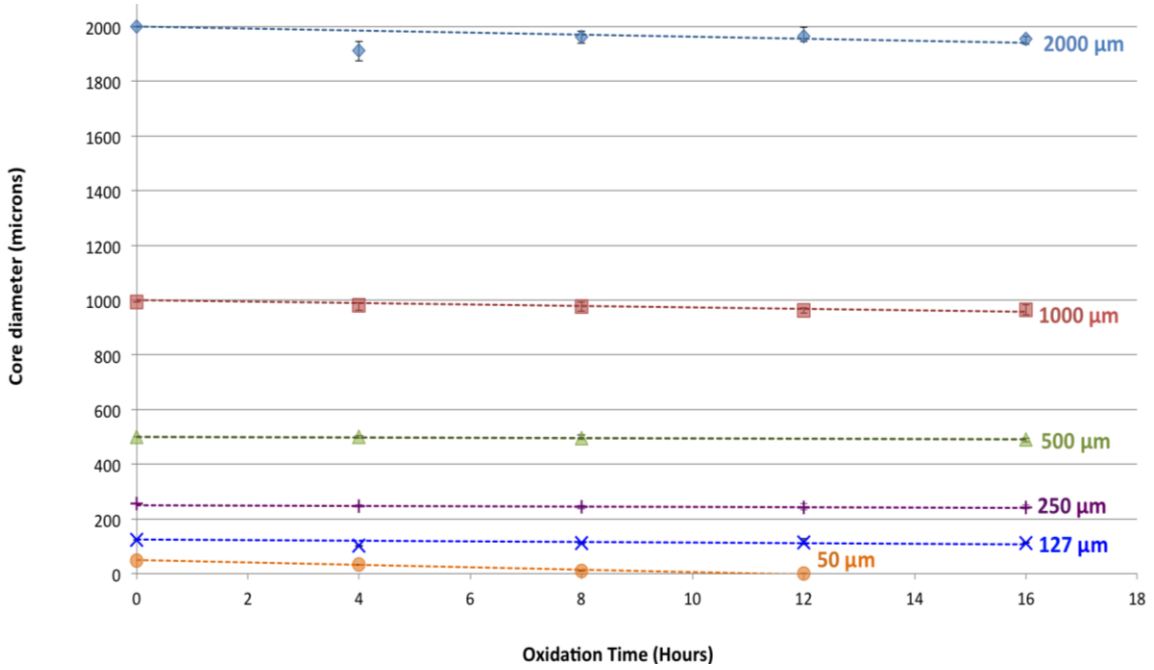

Figure 9: A plot of residual core diameter vs. time for samples exposed to Ar-20% O_2 at 800°C. The dashed lines represent the linear fit for the decreasing core diameter values.

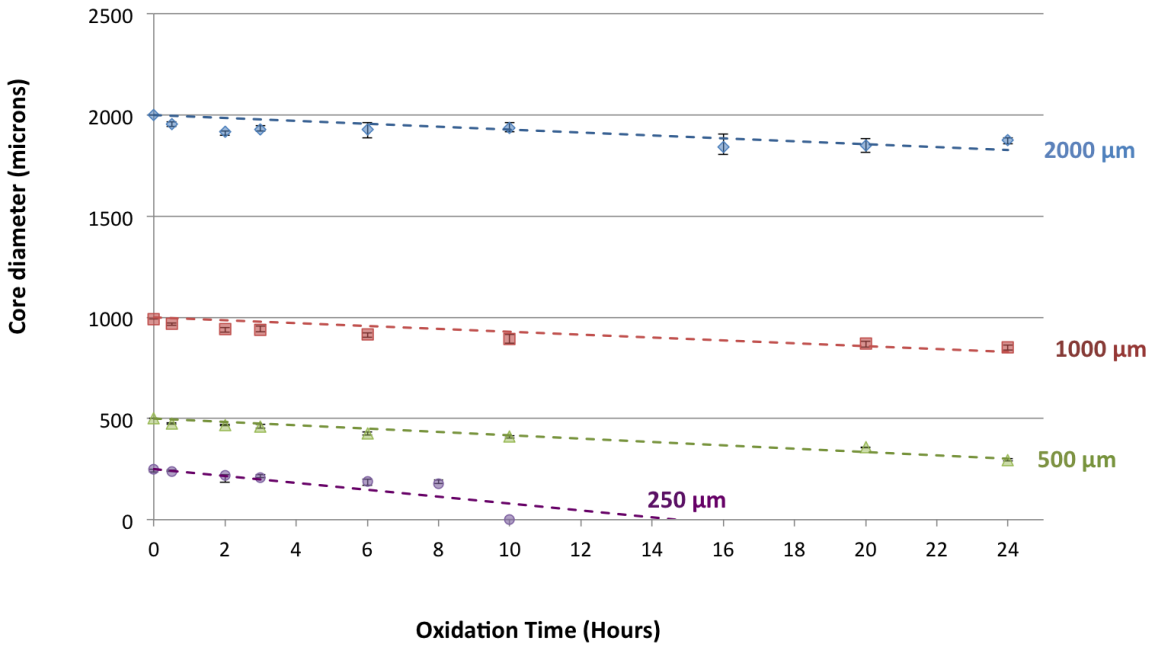

Figure 10: A plot of residual core diameter vs. time for samples exposed to Ar-20% O_2 at 1000°C.

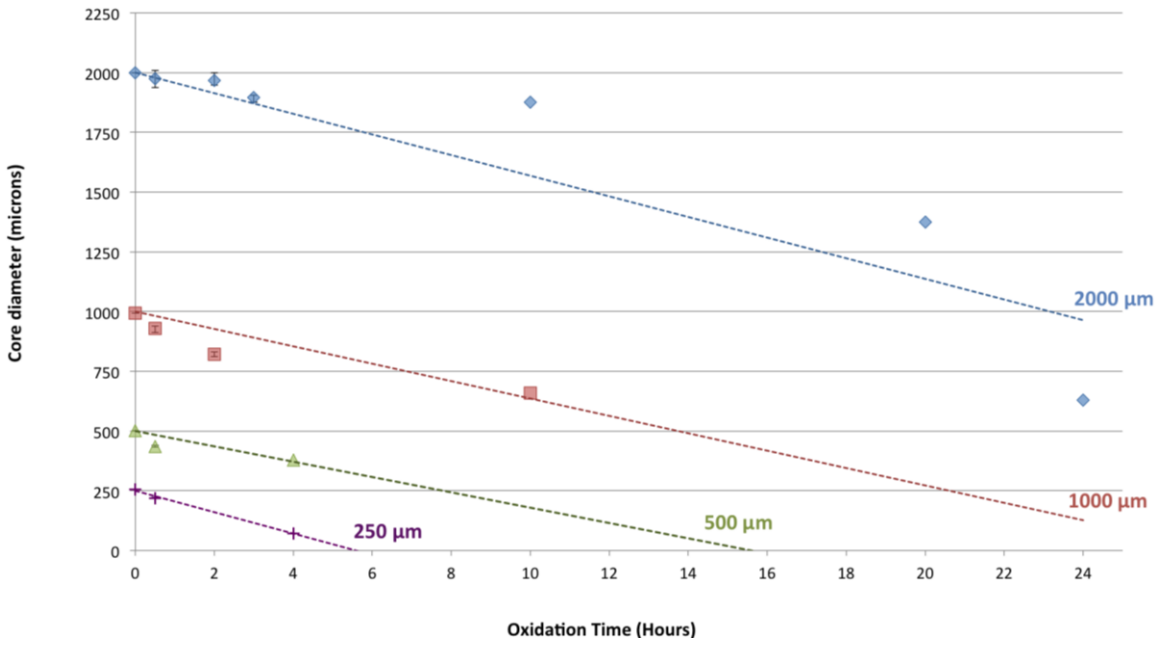

Figure 11: A plot of residual core diameter vs. time for samples exposed to Ar-20% O_2 at 1200°C

It can be observed from the above data that the decrease in the residual core diameter was larger with a smaller initial diameter of the sample and a higher temperature of oxidation.

The above-obtained values of core diameter measurements were used further to fit the data in an oxidation kinetics model for cylindrical geometry and calculate the reaction rate constants and the activation energy for oxidation, which are discussed in the Discussion section.

It is worth noting that the optical micrographs showing the morphology (for example, in Figure 28 as discussed later) suggested that these residual cores were oxygen saturated, meaning that besides oxide scale formation the Ti wires also underwent oxygen dissloution. Thus, the core diameter measurements could also be helpful in drawing some conclusions regarding the kinetics of oxygen dissolution in the Ti metal.

4.2 Comparison of Oxidation Behavior in Ar-20% O_2 and N_2-20% O_2

Most of the oxidation studies on the effect of different oxidizing environments on titanium have only been carried out on planar geometry and negligible work has been done on cylindrical or other non-planar geometries. Hence, present work was also aimed at assessing the effect of Ar-20% O_2 and N_2-20% O_2 on the oxidation behavior of titanium wires.

To have a detailed comparison between oxidation in Ar-20% O_2 and N_2-20% O_2, 5-7 different samples of 250 μm and 500 μm diameter Ti wire were oxidized first in an Ar-20% O_2 atmosphere at 1000°C for 8 hours and the experiment was repeated with identical conditions for oxidation in a N_2-20% O_2 atmosphere. The data for oxide thickness and residual core diameter obtained was used to compare the oxidation behavior between the two oxidizing environments. The plot of oxide thickness vs. time providing such comparison for 250 μm and 500 μm diameter samples is shown in Figure 12 and Figure 13, respectively.

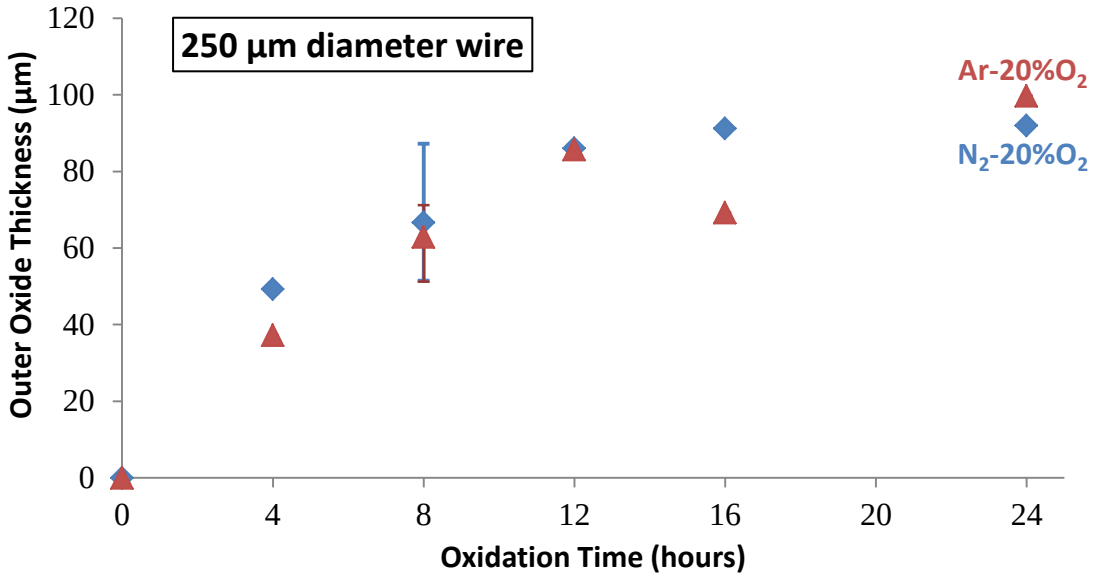

Figure 12: A comparative plot for outer oxide thickness vs. time for 250 µm diameter samples oxidized at 1000°C for 8 hours under identical conditions in Ar-20% O_2 and N_2-20% O_2, respectively.

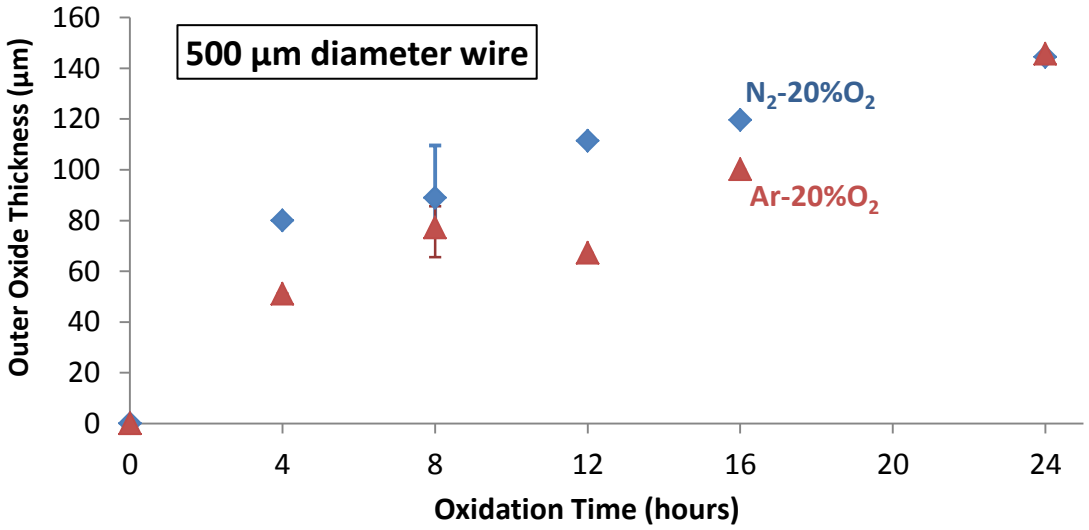

Figure 13: A comparative plot for outer oxide thickness vs. time for 500 µm diameter samples oxidized at 1000°C for 8 hours under identical conditions in Ar-20% O_2 and N_2-20% O_2, respectively.

The data points at 8 hours of oxidation on the above two plots represent the average value of oxide thickness measurements of 5-7 different samples and the error

bars represent the maximum and minimum values of oxide thickness from the set of these 5-7 samples. The data points at 4, 12, 16, and 24 hours of oxidation in each plot were obtained by measurements on just one sample (instead of multiple samples). Hence, the error bars for those data points are not represented.

Plots for core radius measurements under similar oxidizing conditions are shown in Figure 14.

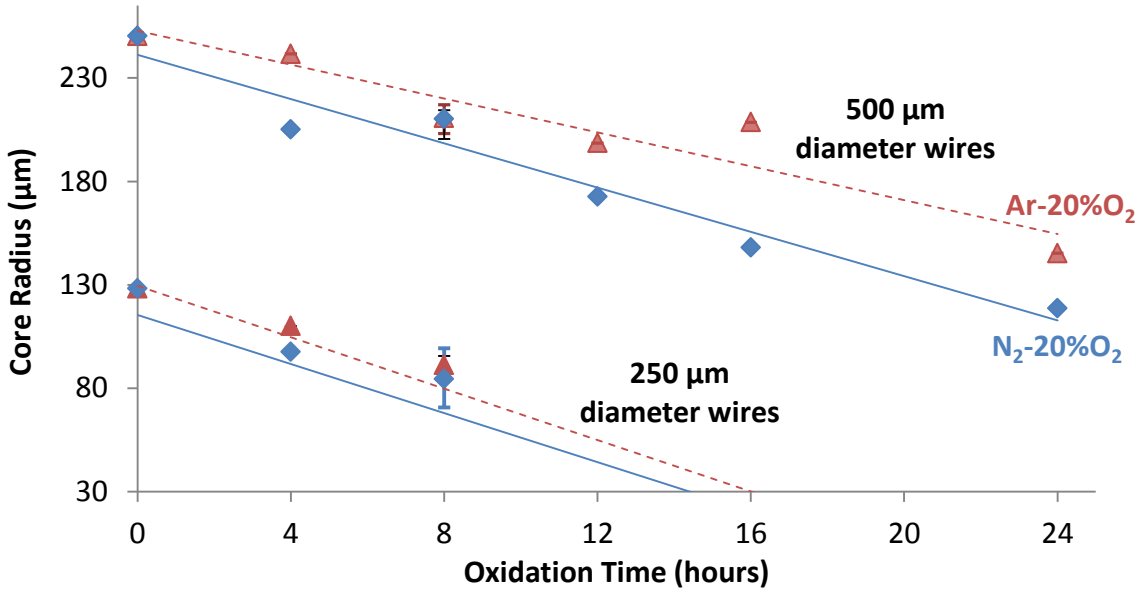

Figure 14: A comparative plot for residual metal core diameter vs. time for 250 µm, and 500 µm diameter samples oxidized at 1000°C for 8 hours under identical conditions in Ar-20% O_2 and N_2-20% O_2. The straight lines in the plot represent linear fit for similar data points.

It can be inferred from Figure 12 and Figure 13 that the oxide thickness in the two environments is almost similar with a slightly increased thickness for oxidation in N_2-20% O_2 than in Ar-20% O_2. As shown in Figure 14, the residual core radius measurements were also similar in the two environments, with the metal core being slightly more utilized upon oxidation in N_2-20% O_2 than in Ar-20% O_2.

These data of oxide thickness and core diameter suggest that there is not much of an apparent difference in the extent of oxidation of samples when oxidized in either N_2-20% O_2 or Ar-20% O_2; however, the extent being a little higher in N_2-20% O_2 than that in Ar-20% O_2. The above-obtained data of core radius measurements along with the data obtained from other samples oxidized at 1000°C in the two environments (as indicated in the sample preparation matrix in Table 1) was further used for calculating and comparing reaction rate constants, which is discussed in the Discussion section (5.2.1).

500 μm diameter samples oxidized under identical conditions in Ar-20% O_2 and N_2-20% O_2 were also characterized using TEM to assess any difference in phases formed, the results of which are reported in the next sub-section.

4.3 TEM Characterization of the Oxidized Titanium Wire

Due to the relatively small size of the samples used and only a trace amount of different phases forming at different locations in the oxidized samples, the characterization results from TEM proved to be substantially important in an analysis of the phases in the oxidized samples. Extensive characterization using TEM was carried out on 3 different samples as listed below:

- 500 μm titanium wire oxidized in Ar-20% O_2 at 1000°C for 8 hours,
- 500 μm titanium wire oxidized in N_2-20% O_2 at 1000°C for 8 hours, and
- 2000 μm titanium wire oxidized in N_2-20% O_2 at 1200°C for 16 hours.

The TEM characterization results for each sample listed above are provided in detail in the following sub-sections.

4.3.1 Characterization of a 500 µm Wire Oxidized in Ar-20% O_2 at 1000°C for 8 Hours

The TEM sample preparation for this oxidized wire was carried out using the TEM sample preparation technique mentioned in the Experimental Procedures section (3.2). The TEM sample had specific locations near the outer oxide and near the metal core, which were thin enough to obtain bright field images and diffraction patterns. The diffraction patterns obtained from different locations of the sample (as pointed on its optical image), along with their indexing and the phases analyzed are shown in Figure 15. The region adjacent to the metal core was analyzed as Ti_2O with hexagonal structure while the outermost region of the oxide was analyzed as TiO_2 (Rutile) with body centered tetragonal (BCT) structure suggesting an increase in the concentration of oxygen from the core of the sample to the outer periphery. Indexing of the diffraction pattern for Ti_2O phase was done by correlating the lattice parameter values from work by Andersson *et al.* [15], while that for TiO_2 (Rutile) by using the values from Rohrer [44], and for $Ti_{0.912}O_2$ from Sanchez *et al*. [45].

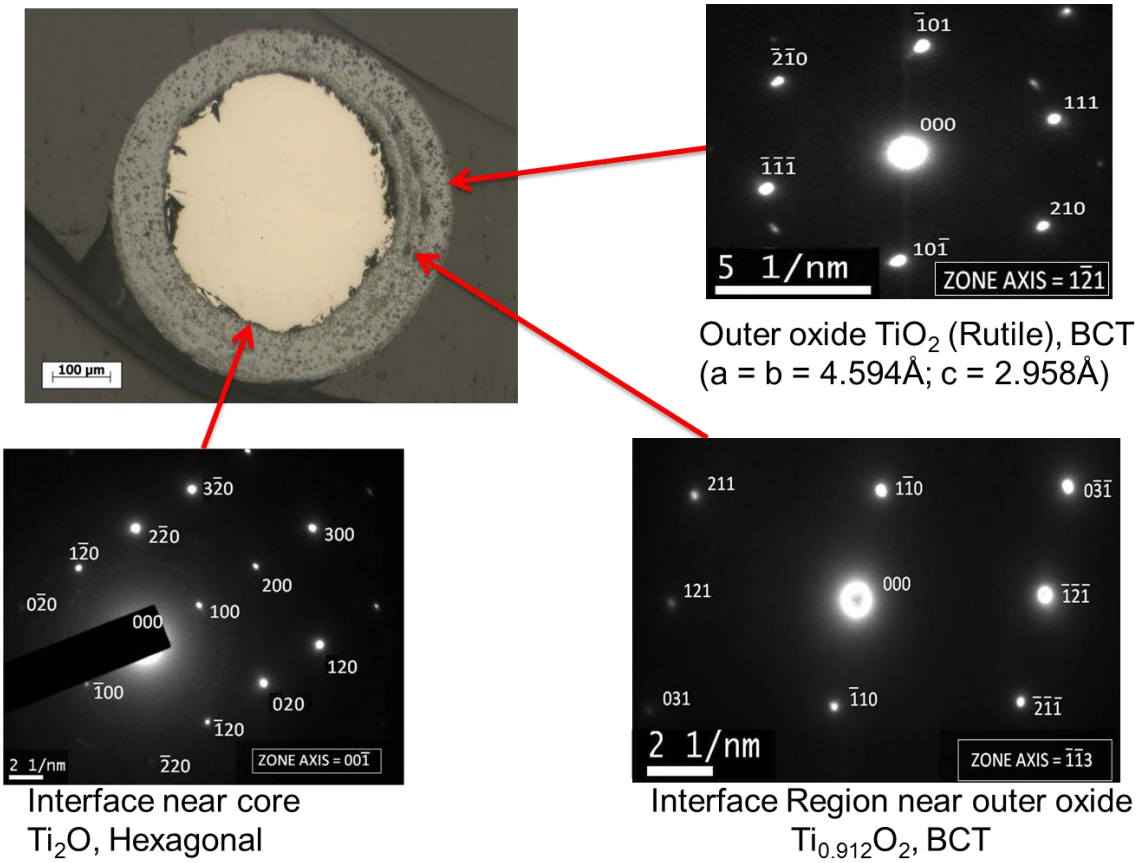

Figure 15: Diffraction patterns (b), (c), and (d) obtained from different regions of oxide scale from the 500 µm titanium wire oxidized in Ar-20% O_2 at 1000°C for 8 hours as indicated in the optical micrograph in (a). The region adjacent to the metal core was analyzed as Ti_2O with hexagonal structure while the outermost region of the oxide was analyzed as TiO_2 (Rutile) with body centered tetragonal (BCT) structure.

4.3.2 Characterization of a 500 µm Wire Oxidized in N_2-20% O_2 at 1000°C for 8 Hours

This sample was analyzed to determine the presence of a nitride layer and, if present, its location in the sample and compare the location of the phases present with that of the 500 µm titanium wire oxidized in Ar-20% O_2 at 1000°C for 8 hours.

- Analysis of the Outer-Most Oxide Scale Region:

  Analysis of the outermost oxide scale was carried out by obtaining a TEM sample in the same way as described in the Experimental Procedure section (3.2). The bright

field images and the (indexed) diffraction pattern obtained from the outermost oxide regions of the TEM sample are shown in Figure 16. The analysis data suggested the outer-most oxide scale to be a TiO_2 phase with body centered tetragonal (BCT) structure.

- Analysis of the Metal-Oxide Interface Region:

  An analysis of the metal-oxide interface region was carried out by obtaining two TEM samples from two different locations using the focused ion beam (FIB) technique. The exact locations from where these TEM samples were prepared using FIB are shown on the SEM images in Figure 17 (a) and (b). Figure 17 (c) and (d) show bright field TEM images of the FIB samples obtained from those locations. Diffraction patterns were obtained from various regions of the FIB sample 1 (FIB sample numbers are marked in Figure 17 (b)). The locations from where these diffraction patterns were obtained from the FIB sample 1, the indexing, and the phase determined are shown in Figure 18. The indexing for the diffraction pattern for TiN was done using values from Rohrer [44] while other phases were indexed using the same references as cited earlier in Section (4.3.1). The indexing of FIB sample 1 suggested a presence of a Ti_2O phase towards the oxide side of the interface, a presence of a TiN phase just adjacent to the interface in the metal core region, and a presence of Ti_2O phase besides the TiN phase, further towards the metal core region.

Subsequently, the diffraction patterns obtained from FIB sample 2 were indexed and the phases determined along with their locations on the sample are shown in Figure 19. Indexing of the diffraction patterns obtained from FIB sample 2 suggest that the

region of the core near the metal-oxide interface area is oxygen rich with the presence of a phase like Ti_3O and Ti_2O.

Thus, the TEM analysis of the 500 μm wire oxidized in N_2-20% O_2 at 1000°C for 8 hours suggested a presence of the following phases:

- TiO_2 in the outermost region of the oxide scale,
- Ti_2O in the scale at the region adjacent to the metal-oxide interface,
- TiN in the metal core region adjacent to the metal-oxide interface, and
- Oxygen rich titanium in the metal core region near the metal-oxide interface.

Figure 20 shows a SEM image summarizing all the phases determined at various locations of the sample using TEM analysis.

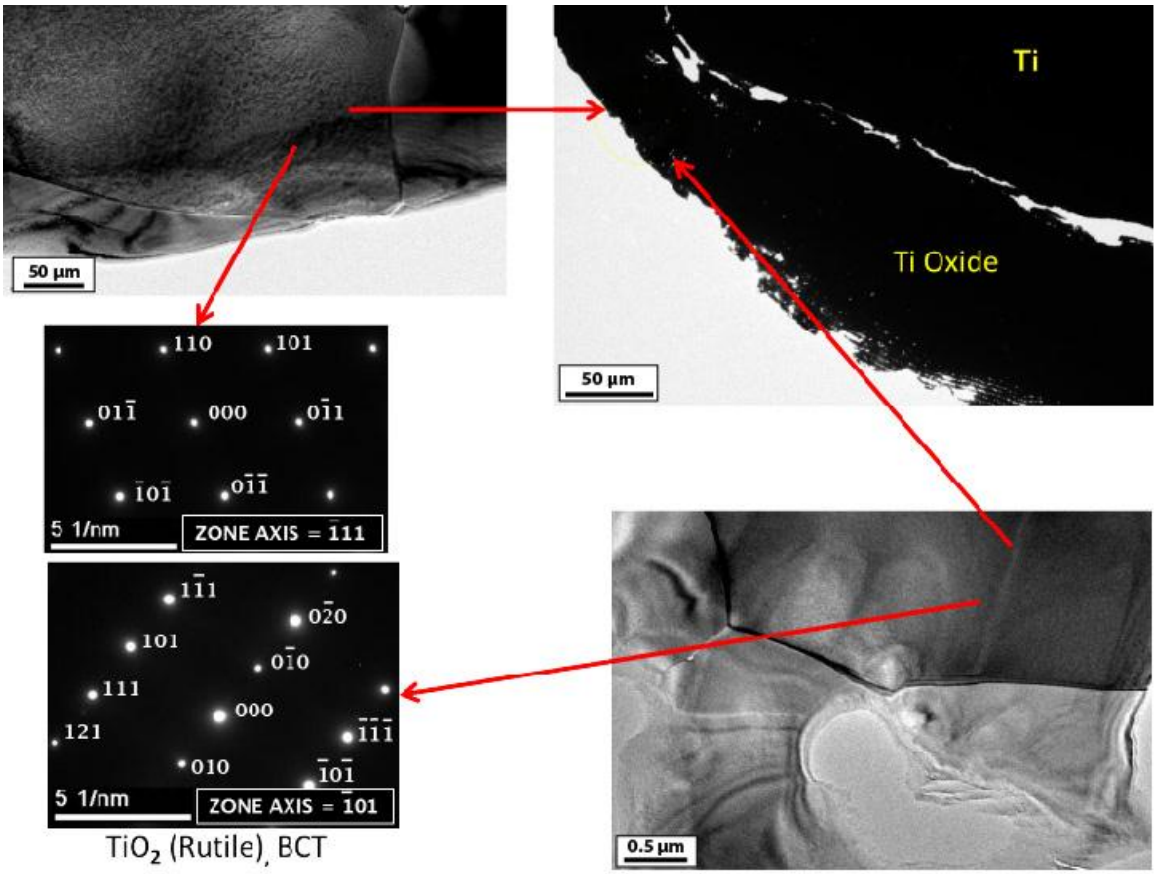

Figure 16: The bright field TEM images and the diffraction patterns obtained from the outer-most oxide region of the 500 µm titanium wire oxidized in N_2-20% O_2 at 1000°C for 8 hours. The indexing of the diffraction patterns revealed the outermost oxide region to be TiO_2 (Rutile).

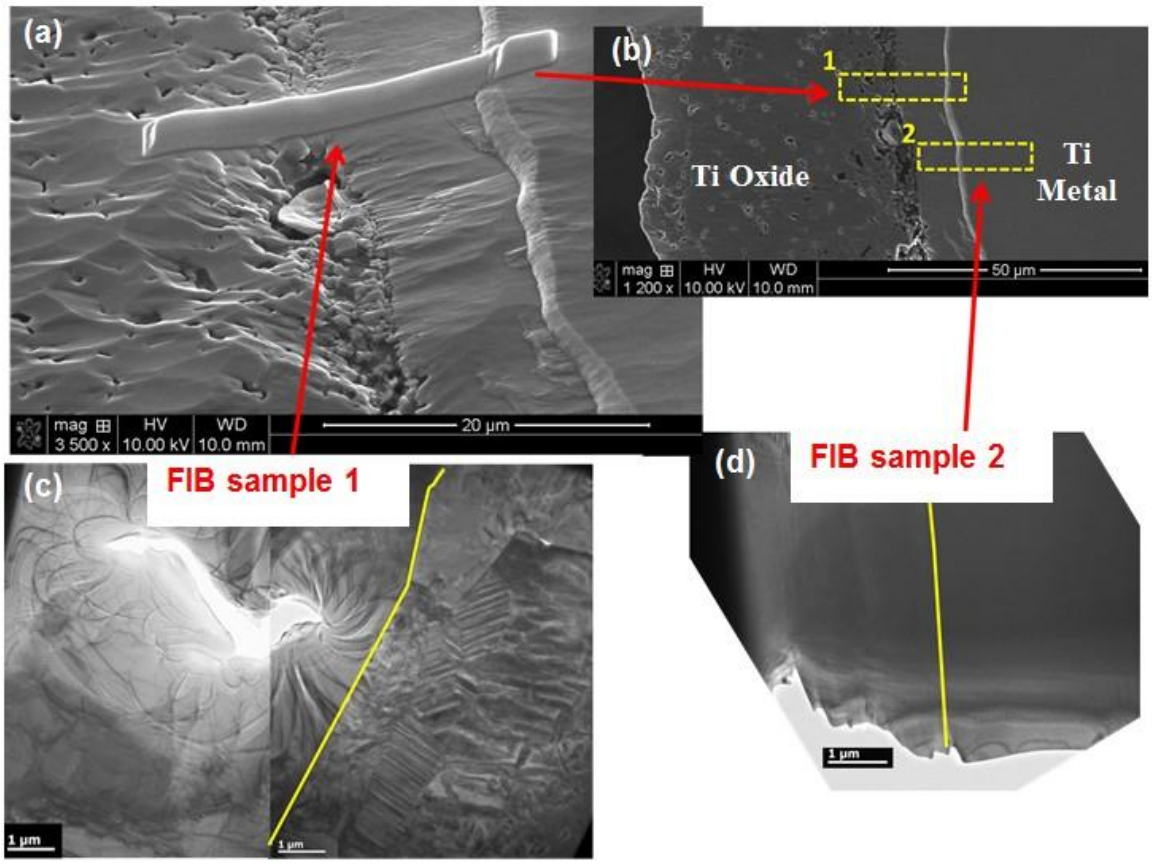

Figure 17: (a) A SEM image showing the Pt marker at the location from where the FIB sample 1 was obtained. (b) A SEM image of the 500 µm titanium wire oxidized in N_2-20% O_2 at 1000°C for 8 hours showing the positions of the 2 FIB samples obtained. (c) and (d) are the TEM bright field images of the two FIB samples obtained from this 500 µm wire. The solid yellow line in both the bright field images indicates an interface boundary.

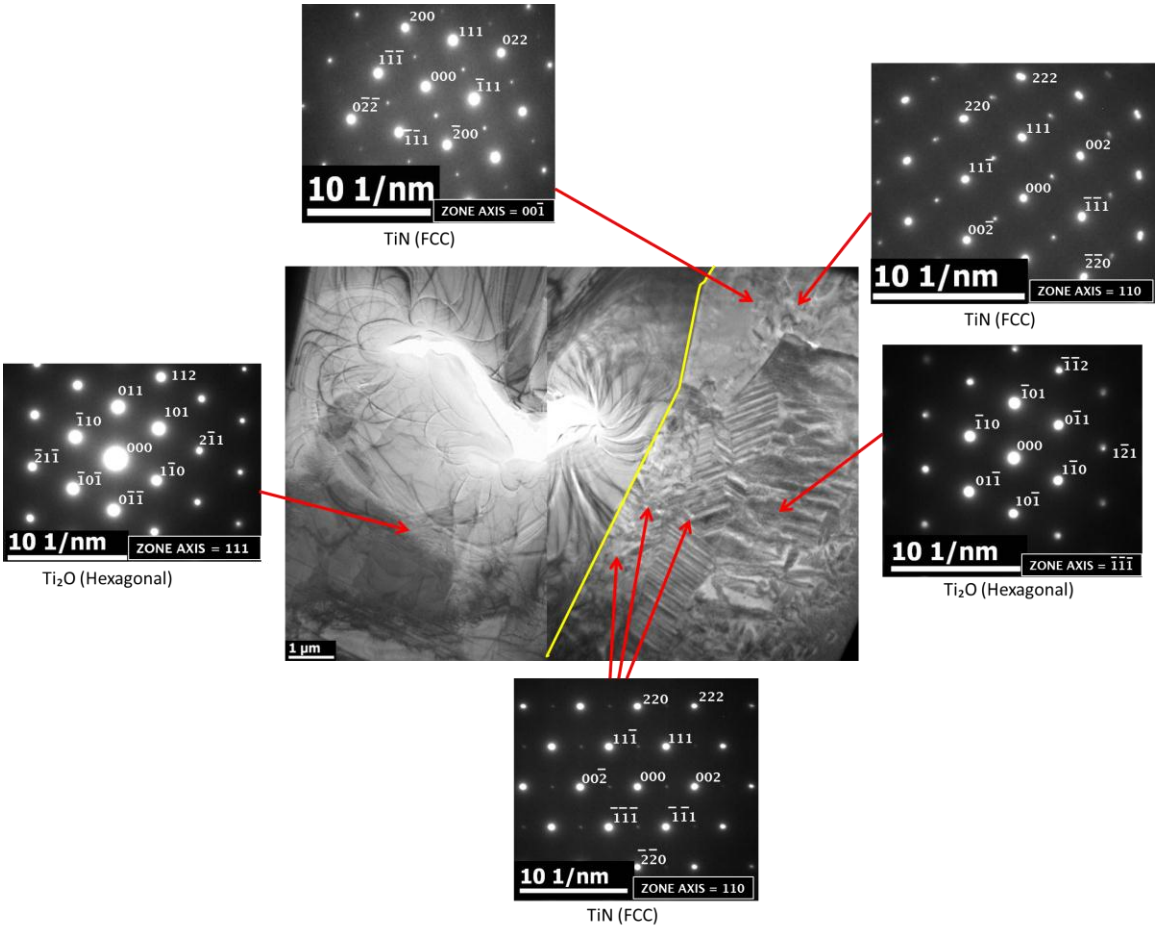

Figure 18: Indexed diffraction patterns obtained from various regions of the FIB sample 1 of the 500 µm titanium wire oxidized in N_2-20% O_2 at 1000°C for 8 hours. The indexing of the diffraction patterns suggests that the region next to the interface towards the oxide scale is Ti_2O and the region on the other side of the interface is TiN. Towards the core of the samples, oxygen rich titanium with a phase similar to Ti_2O is found to exist.

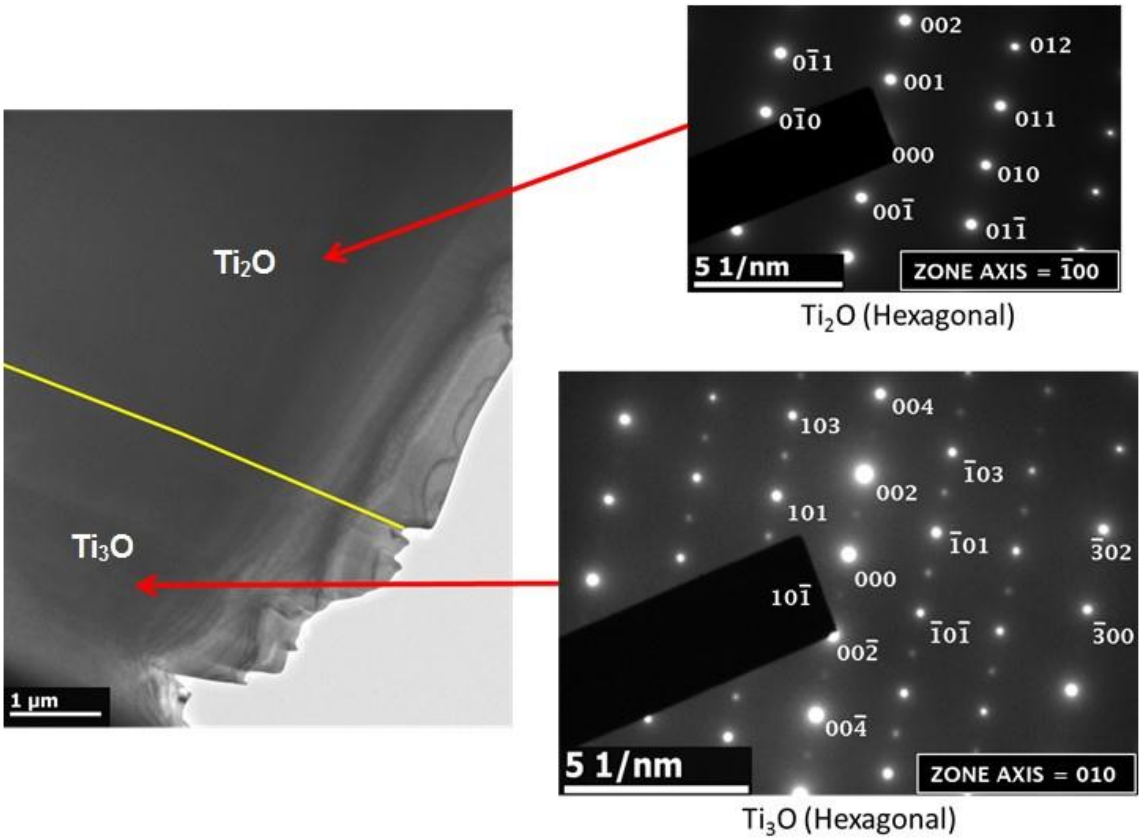

Figure 19: Indexed diffraction patterns obtained from two regions separated by an interface boundary (shown in yellow) of the FIB sample 2 of the 500 µm titanium wire oxidized in N_2-20% O_2 at 1000°C for 8 hours. The indexing of the diffraction patterns suggests that the region is oxygen rich titanium with a presence of Ti_3O towards the oxide scale and Ti_2O towards the metal core side of the interface.

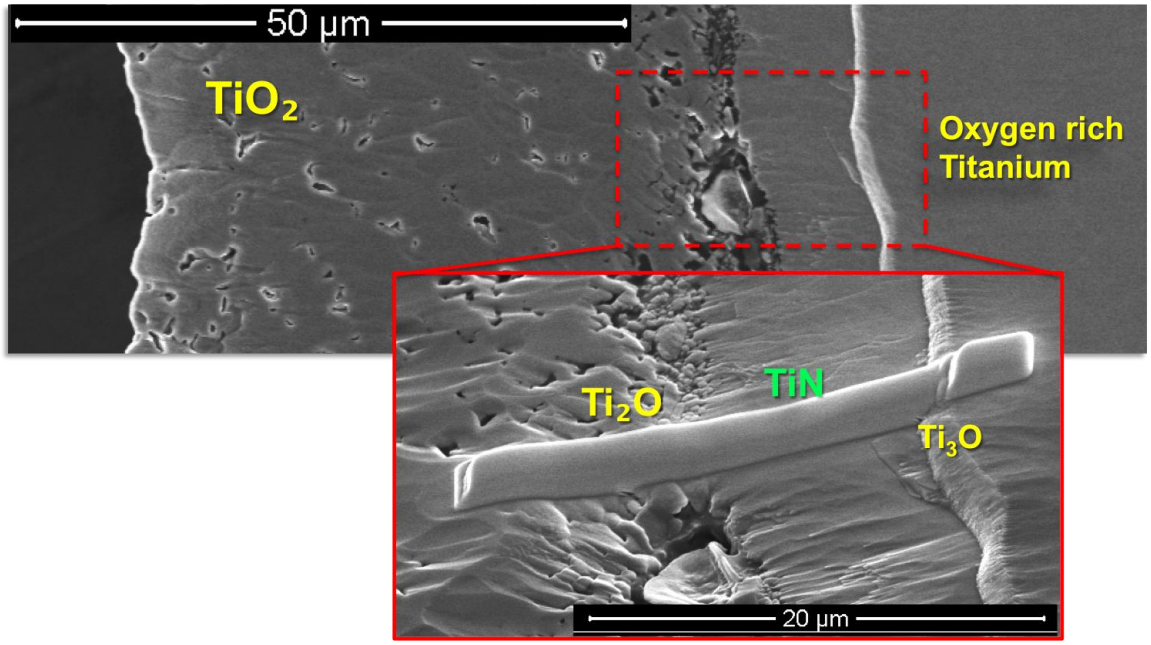

Figure 20: A SEM images of the 500 µm titanium wire oxidized in N_2-20% O_2 at 1000°C for 8 hours indicating various phases determined using TEM analysis at different locations of the sample. The analysis suggested a presence of TiO_2, Ti_2O, TiN, and oxygen rich titanium as moving from the outer oxide region towards the inner core region.

4.3.3 Characterization of a 2000 µm Wire Oxidized in N_2-20% O_2 at 1200°C for 16 Hours

The analysis of this sample was carried out because its optical images showed the presence of layers of oxides with distinct colors as shown in Figure 21. The analysis of this sample was also done by obtaining TEM samples using a similar approach to that for 500 µm titanium wire oxidized in N_2-20% O_2 at 1000°C for 8 hours.

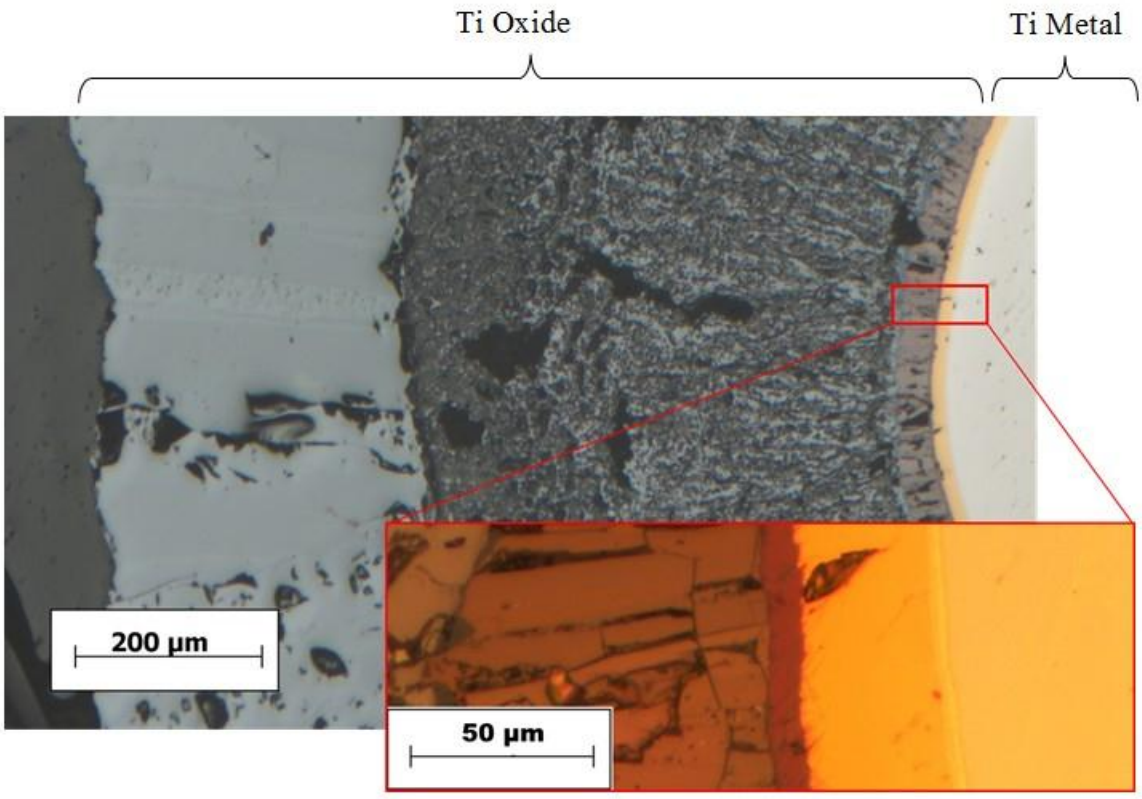

Figure 21: Magnified optical images of 2000 µm titanium wire oxidized in N_2-20% O_2 at 1200°C for 16 hours, showing various distinct oxide layers.

- Analysis of the Outer-Most Oxide Scale:

  The analysis of this region was carried out on a TEM sample prepared using the conventional method as described in Experimental Procedures section (3.2). The TEM bright field images and the corresponding (indexed) diffraction patterns obtained are shown in Figure 22. Since, from all the regions, diffraction patterns with similar indexing were obtained, only a single indexed pattern, suggesting a presence of TiO_2 phase in the outermost oxide, is represented for all the regions.

- Analysis of the Metal-Oxide Interface Region:

  Similar to the sample analyzed in Section (4.3.2), analysis of the metal-oxide

interface region for this sample was carried out by obtaining two TEM samples using FIB. The exact locations from where these samples were prepared are shown on the magnified optical image in Figure 23 (a). Figure 23 (b) and (c) show bright field TEM images of the FIB samples obtained. Since the samples for TEM analysis were obtained from interface regions that were very porous, the samples showed damaged areas separating the phases on either side of the interface. The damaged areas representing the interface boundaries in the samples are shown by dashed yellow line in Figures 23 (b) and (c).

FIB sample 1 was analyzed to have a presence of TiO_2 phase at the outer oxide side of the interface while a presence of Ti_2O phase was towards the inner core side of the interface. Figure 24 shows indexed diffraction patterns and phases determined from two regions separated by an interface boundary of the FIB sample 1.

Figure 25 shows an indexed diffraction pattern suggesting the presence of the Ti_2O phase at the outer oxide side of the interface and probable phases present at the interface and other locations of the FIB sample 2. The probable phases listed at the specific locations were provided in Figure 25 by considering the closeness of the indexing on the diffraction patterns obtained from those regions.

Thus, the TEM analysis of the 2000 μm titanium wire oxidized in N_2-20% O_2 at 1200°C for 16 hours suggested a presence of TiO_2 in the outer-most compact oxide scale, a presence of distinct layers of TiO_2 and Ti_2O in the oxide scale region near the scale-metal interface, and a nitrogen rich region in the metal core region near the interface. Figure 26 shows optical images of the sample with all the phases identified using the TEM analysis.

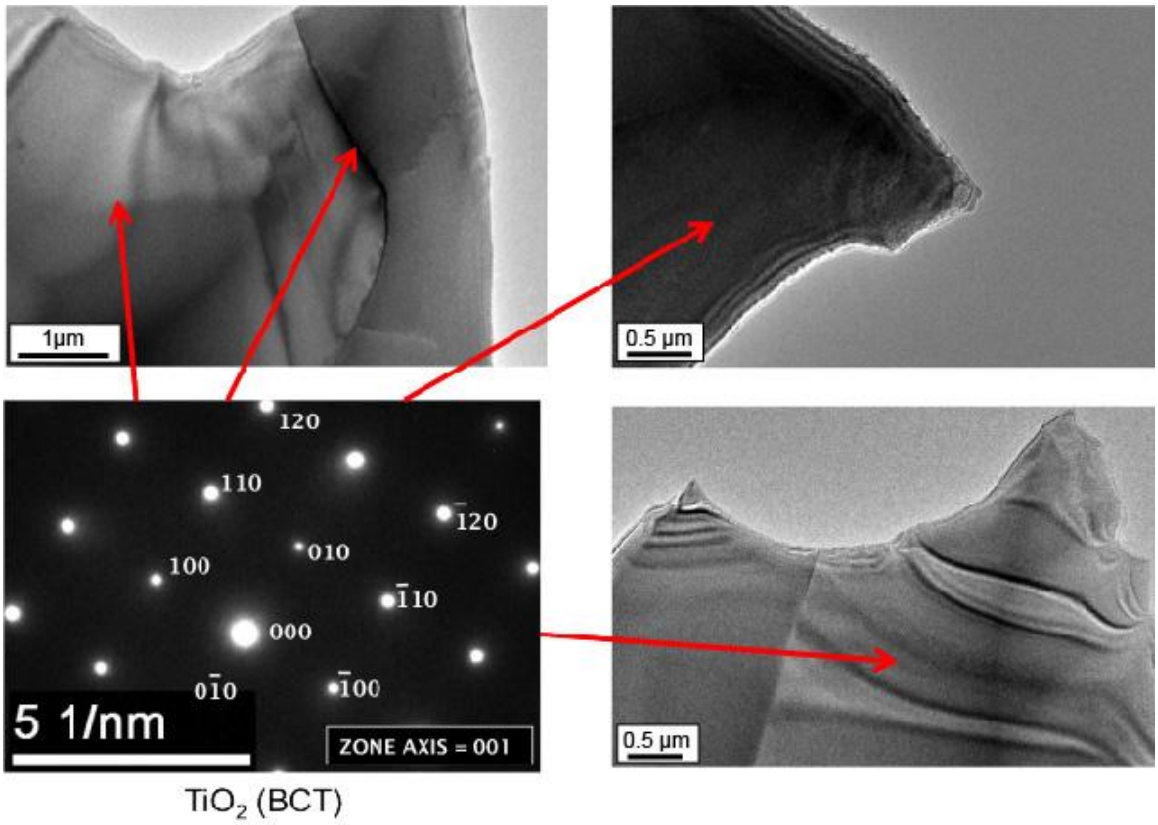

Figure 22: Bright field TEM images and indexed diffraction patterns obtained from the outer-most oxide region of the 2000 µm titanium wire oxidized in N_2-20% O_2 at 1200°C for 16 hours. The diffraction pattern suggests that the outer-most oxide region is essentially TiO_2 (rutile).

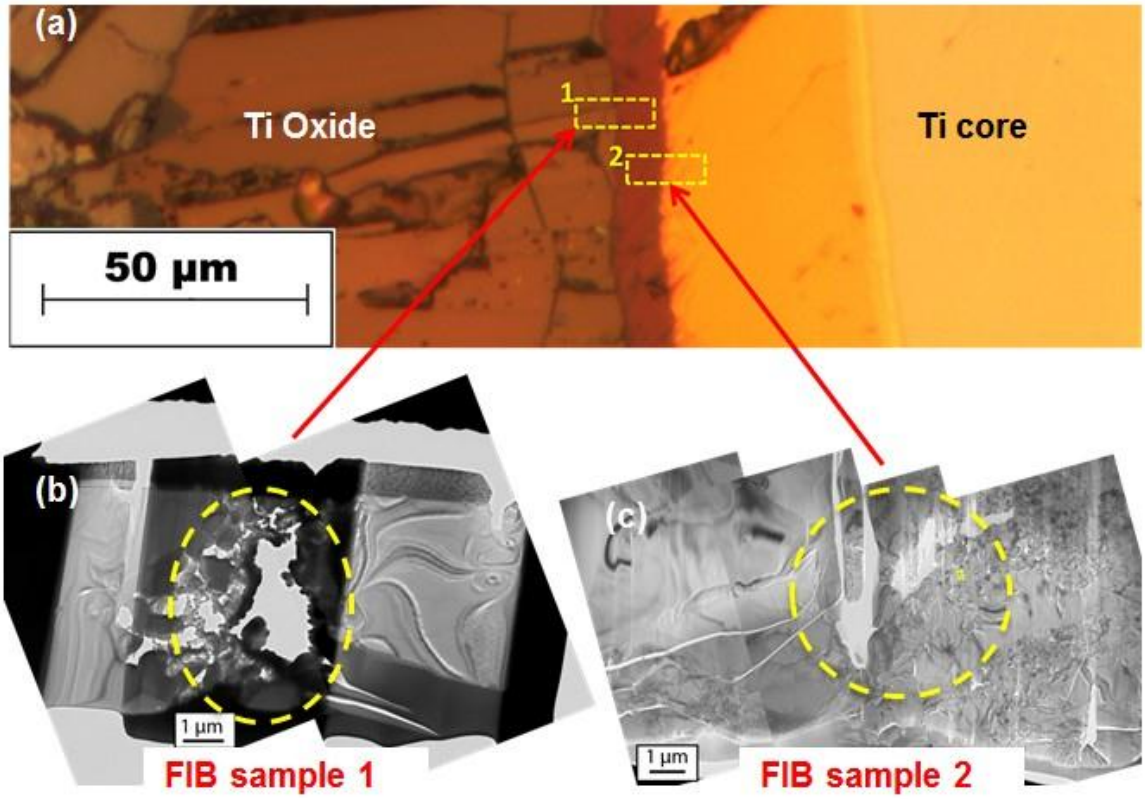

Figure 23: (a) A magnified optical image of the 2000 µm titanium wire oxidized in N_2-20% O_2 at 1200°C for 16 hours showing the positions of the two FIB samples obtained. The FIB samples are marked with numbers 1 and 2. (b), (c) TEM bright field images of FIB sample 1 and 2, respectively. The damaged area/gap in both the bright field images as indicated using dashed yellow lines are the interface boundaries.

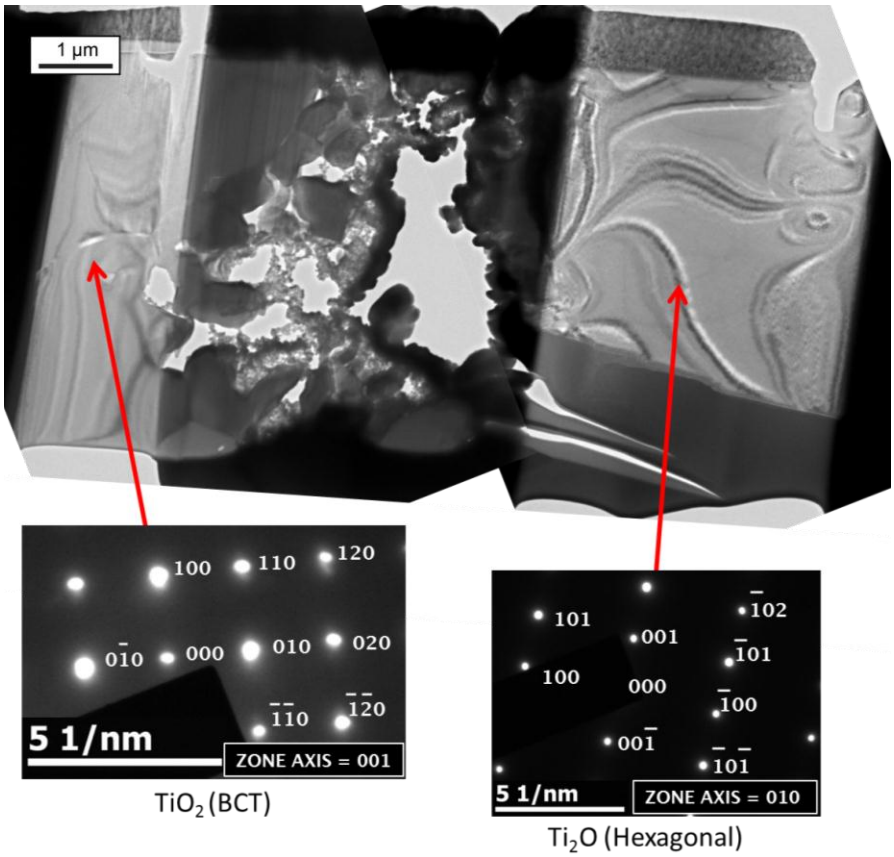

Figure 24: Indexed diffraction patterns obtained from two regions separated by an interface boundary of the FIB sample 1 (as indicated in Figure 21) of the 2000 µm titanium wire oxidized in N_2-20% O_2 at 1200°C for 16 hours. The indexing of the diffraction patterns suggests that the region towards the oxide scale is TiO_2 and the region towards the metal core is Ti_2O.

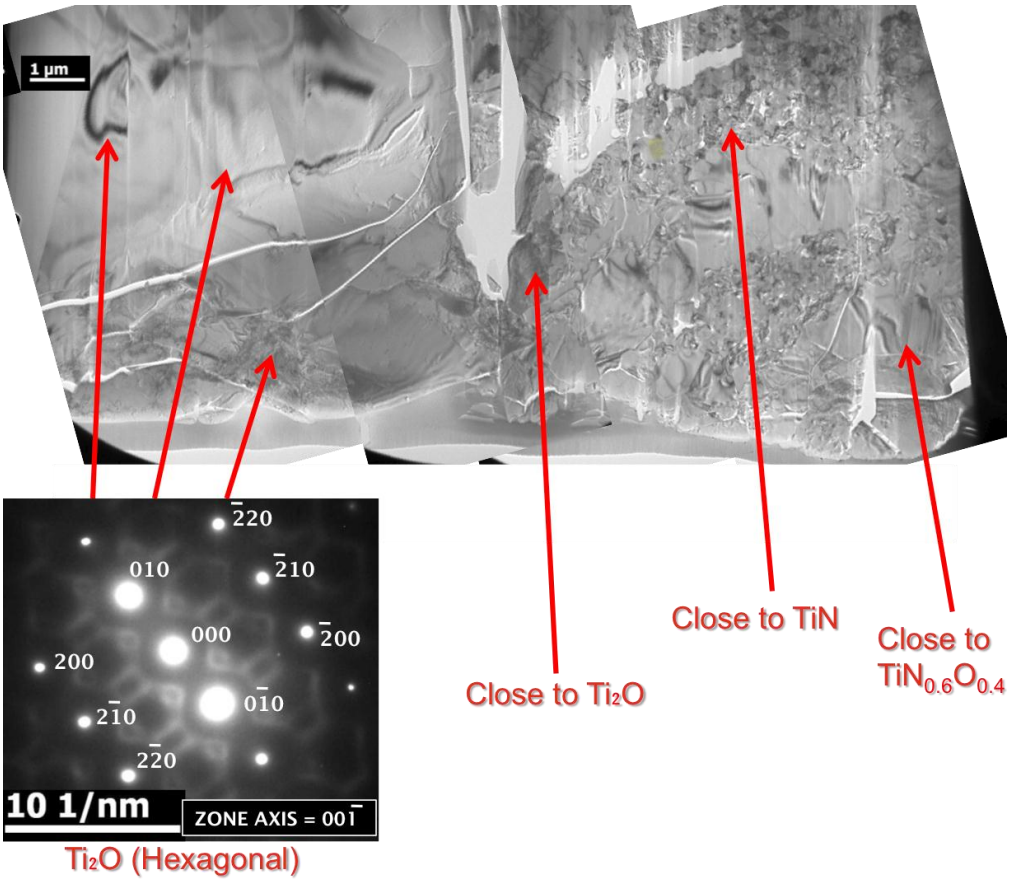

Figure 25: Indexed diffraction patterns obtained from different regions separated by an interface boundary of the FIB sample 2 (as indicated in Figure 21) of the 2000 µm titanium wire oxidized in N_2-20% O_2 at 1200°C for 16 hours. The diffraction patterns suggest that the region towards the oxide scale is Ti_2O and the region towards the metal core consist of nitrogen in varying amounts. The bright field TEM image of the FIB sample 2 shows nucleation of small grains in the regions, which were indexed as phases

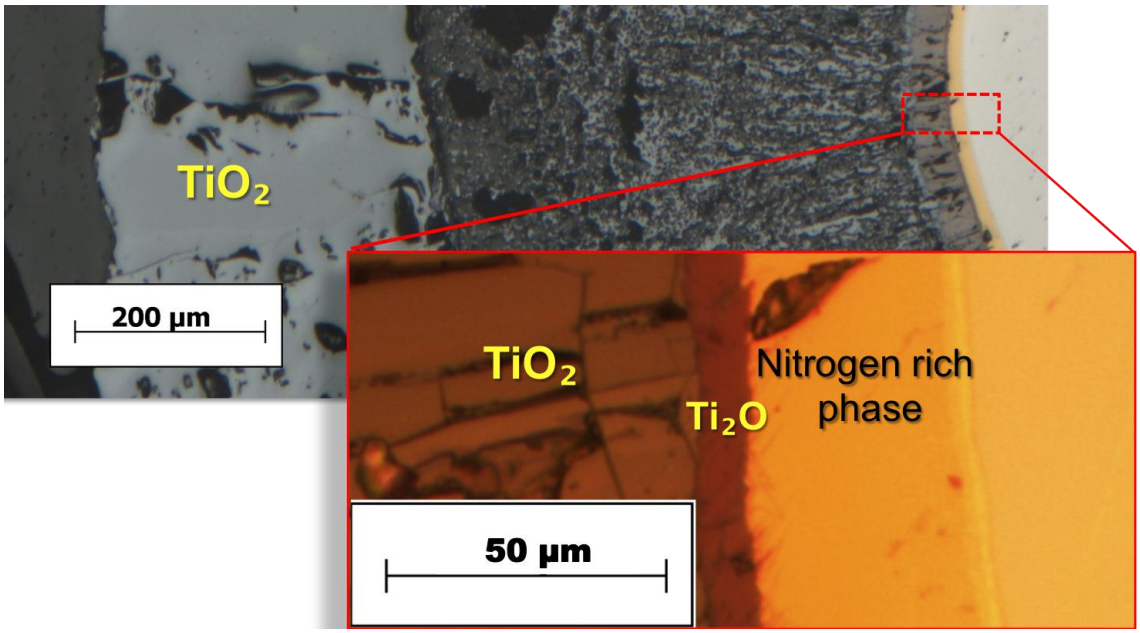

Figure 26: Optical images of the 2000 µm titanium wire oxidized in N_2-20% O_2 at 1200°C for 16 hours indicating the phases identified using TEM analysis. TEM analysis revealed presence of TiO_2 (Rutile) phase in the outer extremities and Ti_2O near the core in the oxide scale. The phase adjacent to the core was analyzed to be rich in nitrogen.

4.4 Morphological Evolution of Oxidized Titanium Wire in Ar-20% O_2

As mentioned in the experimental procedures section, the cross-sections of the oxidized samples were observed under optical microscope and their images were taken. Close observation of a number of such images, arranged in sequence of increasing oxidation time, helped in understanding the morphological evolution of the oxide scale.

The following morphological features were assessed using optical microscopy:

- Oxide Color,
- Surface texture,
- Porosity of the oxide scale,
- Presence of multiple phases and oxide,
- Adherence of the oxide scale to the metal surface, and

- Location, orientation, and direction of propagation of cracks and voids if present in the oxide scale.

All pure titanium wires exhibited a general trend in their morphological evolution with respect to an increasing oxidation time with a few exceptions. Based on the observation of the microstructures, it appeared that the oxidation process occurred in the following steps:

1. The oxidation began with the dissolution of oxygen in the metal core. Once the outer periphery of the core got completely saturated with oxygen, the formation of titanium sub-oxide scale began at the Ti-gas interface. This scale was observed to be grey-black in color during the initial stages.
2. Thereafter, the simultaneous dissolution of oxygen in the core and the formation of oxide scale continue until the sub-oxide scale reached a critical thickness and detached from the core forming TiO_2 layer. A close look at the Ti-O phase diagrams presented in Figure 2 and 3 will help better understand the morphological evolution described so far. With increasing oxygen content from left to right in the Ti-O phase diagram, one can observe an increasing dissolution of oxygen in α-Ti before forming oxide like Ti_3O, Ti_2O, TiO, Ti_2O_3, and TiO_2.
3. The oxide TiO_2 scale appeared white in color after complete detachment from the metal surface. The formation of a new coherent sub-oxide was observed to occur quite uniformly beneath this detached outer scale. It was also observed that further dissolution of oxygen in the metal core continued beneath these oxide scales, hence confirming the porous nature of the oxides. Figure 27 is a good example of the

oxidation stage described in the above steps. Figure 28 shows a magnified image of Figure 27 along with the labeling of phases.

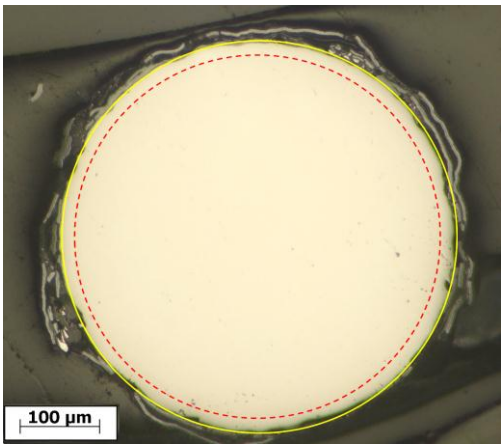

Figure 27: An optical micrograph of a 500 µm diameter titanium wire oxidized at 800°C for 4 hours in Ar-20% O_2 showing multiple layers of the oxide. The yellow solid circle represents the initial diameter of the sample (500 µm) and the dashed red line suggests the extent of oxygen dissolution in the sample.

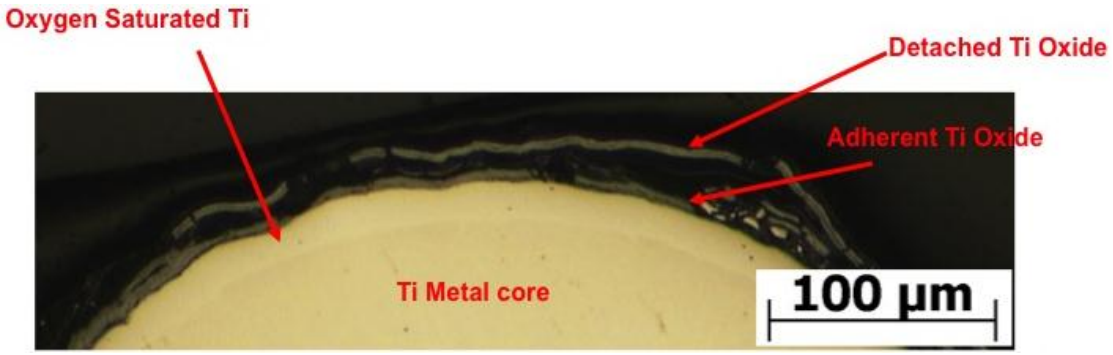

Figure 28: A magnified optical image of 500 µm diameter titanium wire oxidized at 800°C for 4 hours in Ar-20% O_2. The image shows a distinct layer of oxygen dissolved in titanium and layers of adherent and detached oxide scale above it.

4. While the formation of oxide scale with more layers continued, the depth of dissolved oxygen in the metal core kept increasing as can be observed by comparing Figure 27 for 4 hours and Figure 29 for 16 hours of oxidation. This process was observed to

further intensify if the initial size of the sample was smaller. One can deduce such an observation by comparing Figure 29 for 500 µm diameter sample and Figure 30 (a) and (b) for 250 and 127 µm diameter samples.

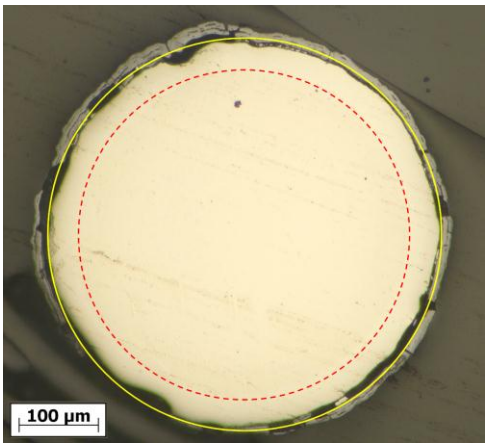

Figure 29: An optical image of 500 µm diameter titanium wire oxidized at 800°C for 16 hours in Ar-20% O_2. The image shows an increased depth of dissolved oxygen in the metal and a thicker oxide scale.

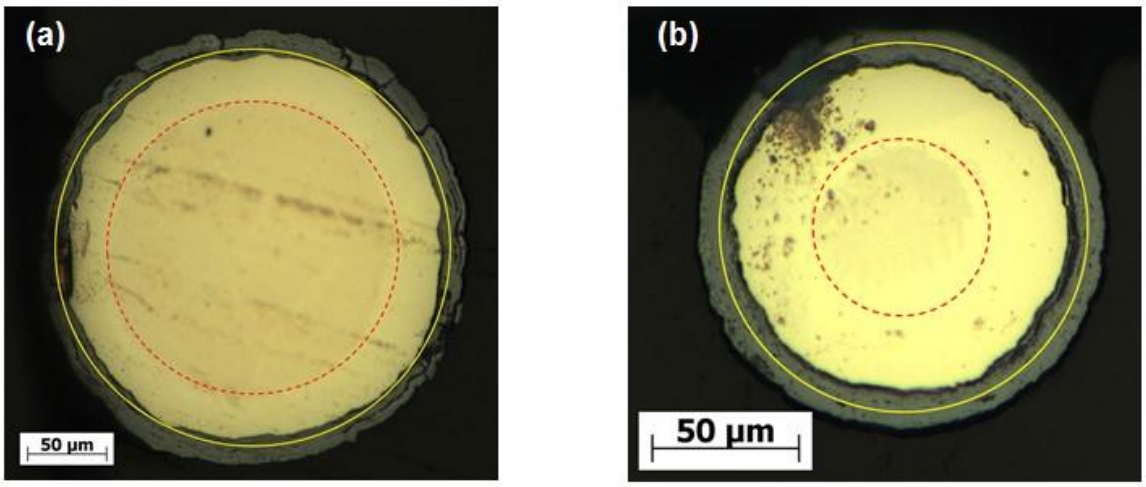

Figure 30: (a) An optical image of 250 µm diameter titanium wire oxidized at 800°C for 16 hours in Ar-20% O_2. (b) An optical image of 127 µm diameter titanium wire oxidized at 800°C for 16 hours in Ar-20% O_2. The images show an increased depth of dissolved oxygen in the metal core and a thicker oxide scale for smaller size samples than the 500 µm sample under similar conditions.

5. When the observation was continued on the 500 µm diameter wire at 1000 °C, the oxide scale consisted of numerous very fine oxide lamellae. This might be because of a very short parabolic oxidation span at 1000 °C (as shown in Figure 4 by Kofstad). Figure 31 shows a micrograph of 500 µm diameter titanium wire oxidized at 1000°C for 30 minutes along with a magnified image showing the fine oxide scale lamellae.

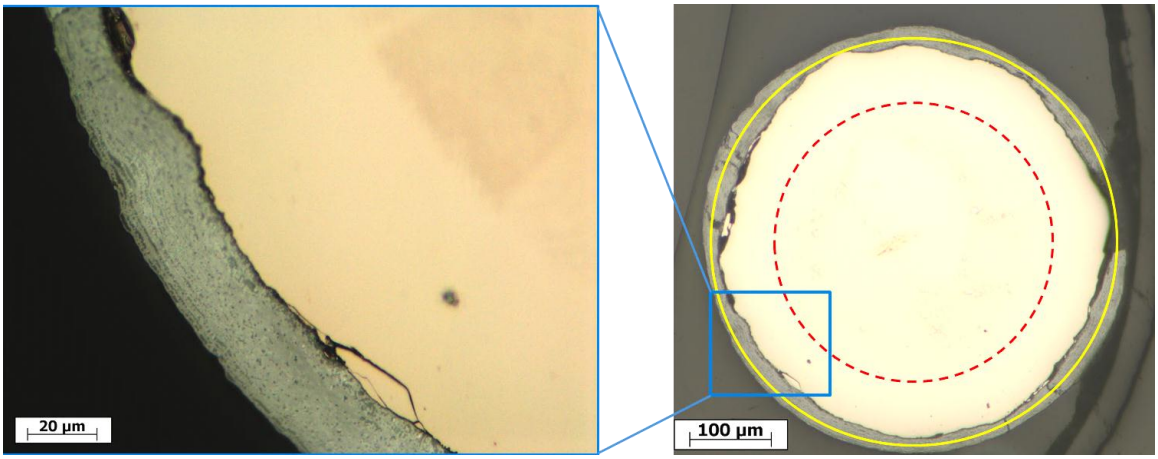

Figure 31: An optical image of 500 µm diameter titanium wire oxidized at 1000°C for 30 minutes in Ar-20% O_2. The image shows an increased depth of dissolved oxygen in the metal and an oxide scale with much finer oxide lamellae.

6. Further oxidation proceeded by the sintering of the fine multi-layers in the oxide scale, resulting in its overall compaction. This process of compaction of the oxide scale continued as the oxidation time increased, eventually resulting in large voids in the oxide scale. Figure 32 demonstrates the compaction of the oxide scale in the 500 µm diameter titanium wire oxidized at 1000°C with increasing oxidation time and appearance of a thin compact outermost oxide scale after 6 hours of oxidation.

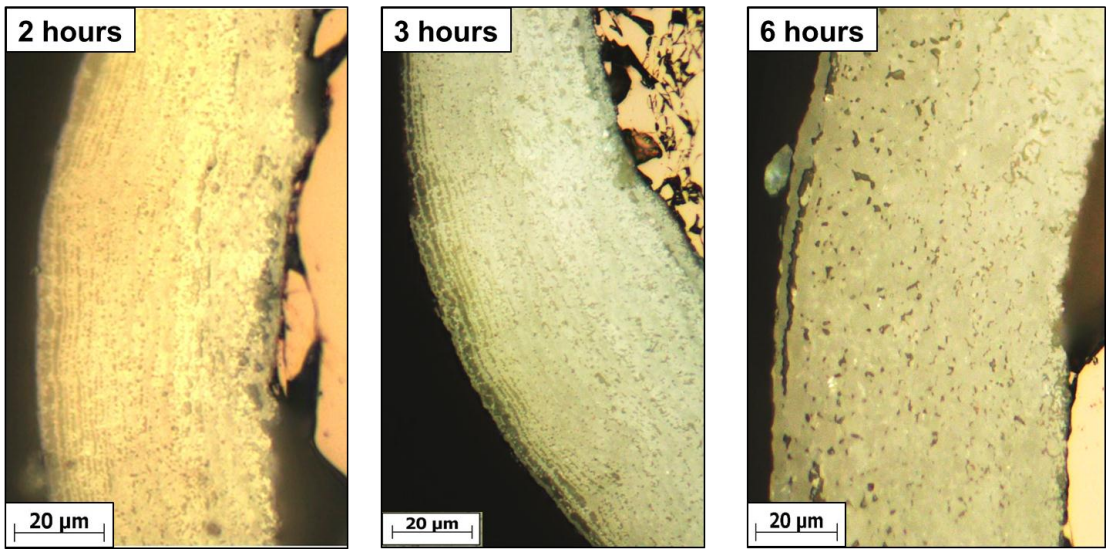

Figure 32: Compaction of the oxide scale with multi-layers with increasing oxidation time as observed in the optical images of 500 µm diameter titanium wire oxidized at 1000°C in Ar-20% O_2. One can observe the formation of a compact outer-most oxide scale at 6 hours of oxidation.

7. Eventually, the outer periphery of the oxide scale was observed to form a distinct, highly compact layer. On the other hand, the scale metal interface exhibited an increasingly porous region that nearly separated the metal core and the oxide scale. Figure 33 shows an increase in thickness of the outer compact oxide scale and the porous interface with even further oxidation in the 500 µm diameter titanium wire oxidized at 1000°C.

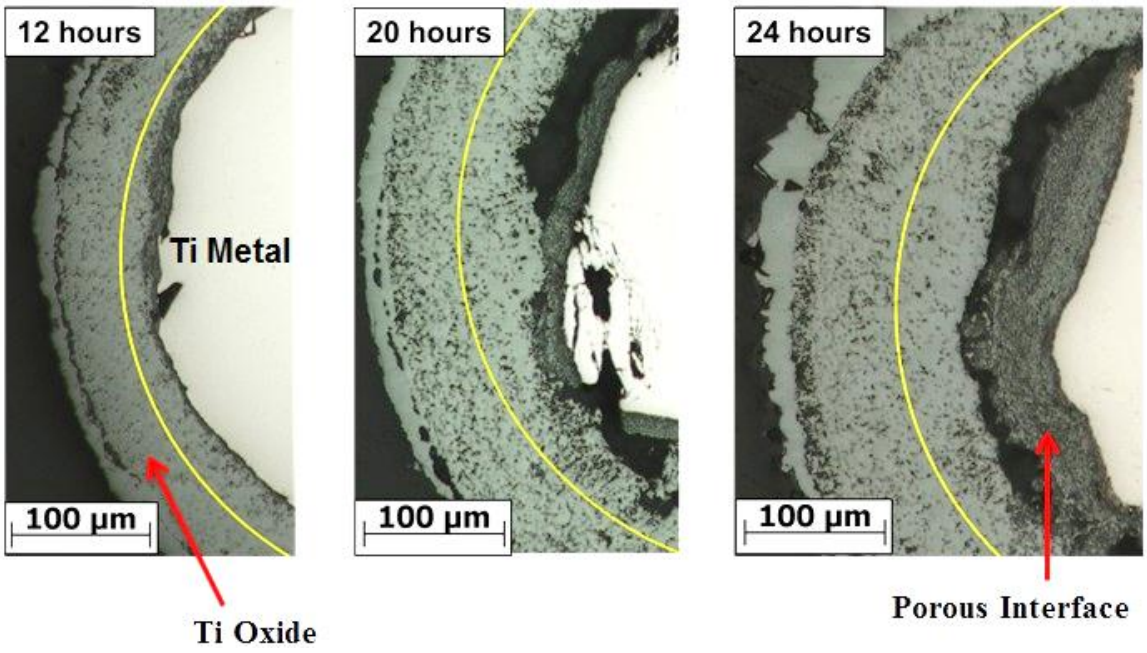

Figure 33: An increase in thickness of the outer compact oxide scale and the porous interface, and further consumption of the oxygen saturated metal core with increasing oxidation time as can be observed (due to increasing distance from the yellow line for original diameter) in the optical images of 500 µm diameter titanium wire oxidized at 1000°C in Ar-20% O_2.

Since the oxidation study was carried out until 24 hours, only further progression of morphology was observed and illustrated using smaller size samples (that is, 250 µm diameter wire) because they undergo a faster oxidation due to their smaller size and more curvature. Figure 34 shows a micrograph of a 250 µm wire oxidized at 1000 ºC for 6 hours representing a morphology similar to that of a 500 µm wire oxidized at 1000 ºC for 24 hours.

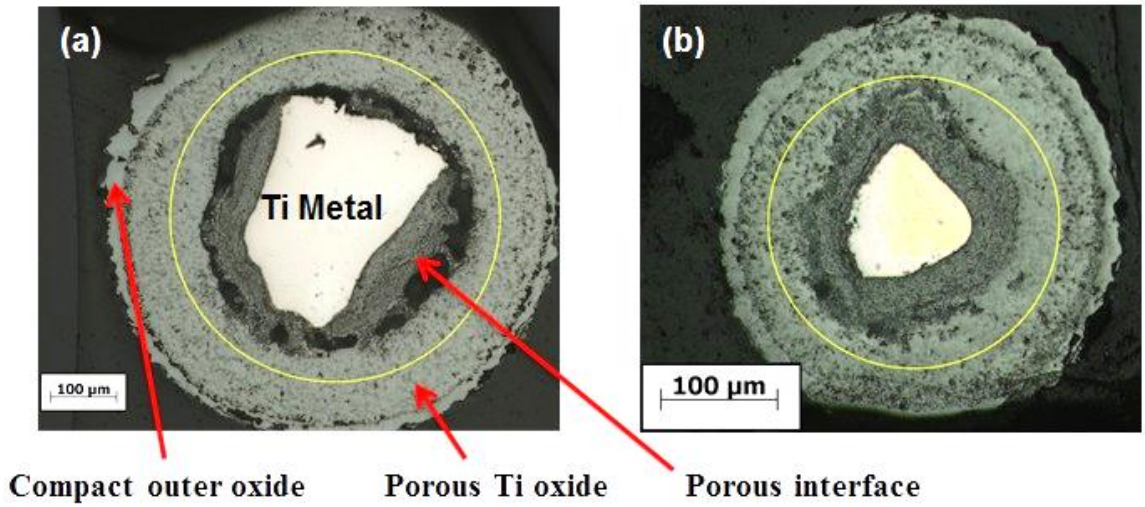

Figure 34: (a) A optical micrograph of a 500 µm wire oxidized at 1000 ºC for 24 hours. (b) An optical micrograph of a 250 µm wire oxidized at 1000 ºC for 6 hours. Both represent a similar stage in the morphological evolution.

8. When the metal core was on the verge of getting completely oxidized, it was observed that the sample exhibited distinct regions that were clearly separated by large circumferential voids. Figure 35 shows a micrograph of a 250 µm wire oxidized at 1000 ºC for 12 hours in which the metal core is almost completely consumed.

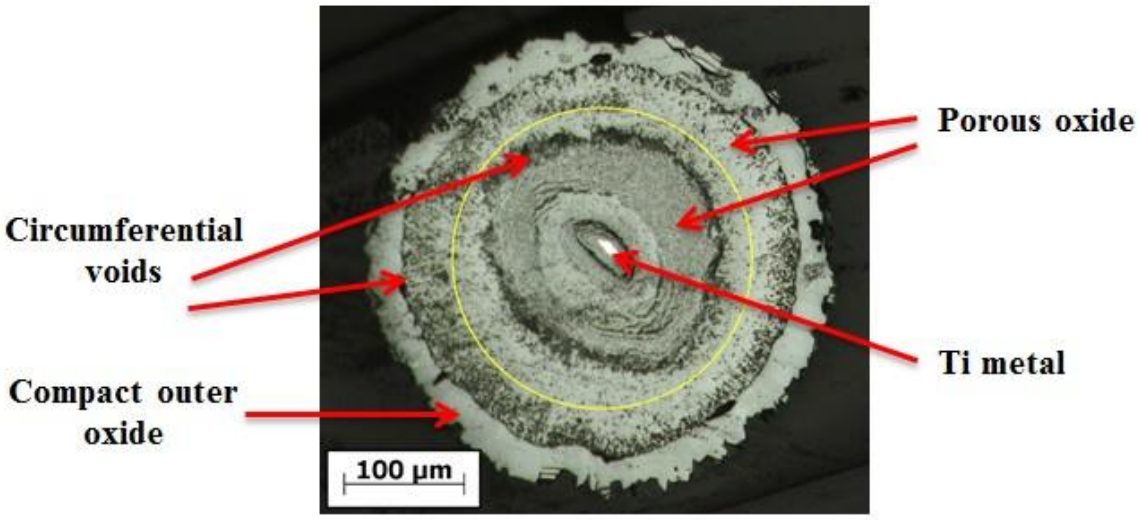

Figure 35: An optical micrograph of a 250 µm wire oxidized at 1000 ºC for 12 hours showing an almost complete metal consumption.

9. Once the metal was completely used up, the oxide scale was observed to consolidate further, resulting in two probable microstructures: (a) a multiple ring-like oxide scale structure shown in Figure 36 or (b) a tube-like oxide scale structure with a hollow core shown in Figure 37.

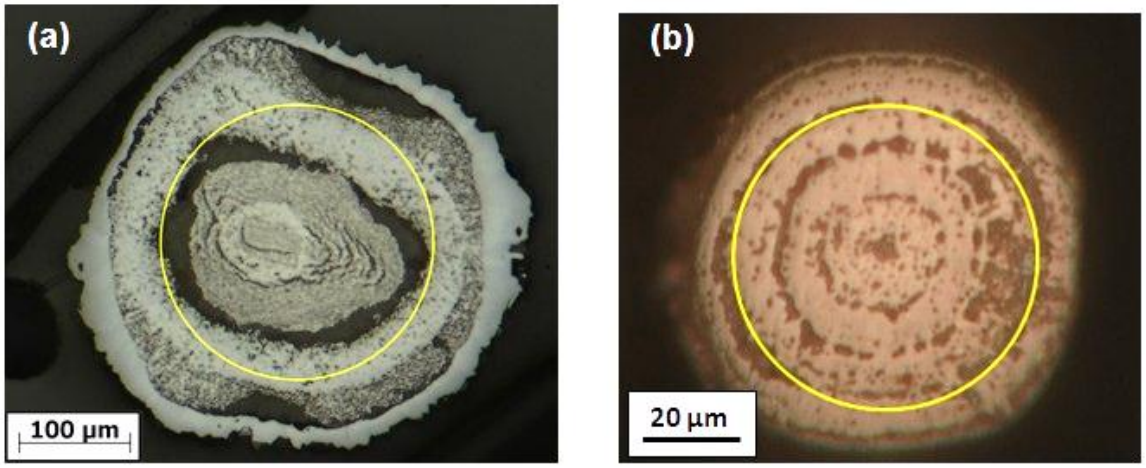

Figure 36: An optical micrograph of (a) 250 µm wire oxidized at 1000 ºC for 24 hours. (b) 50 µm wire oxidized at 1000 ºC for 10 hours. Both micrographs show multiple rings of oxide with large voids separating them.

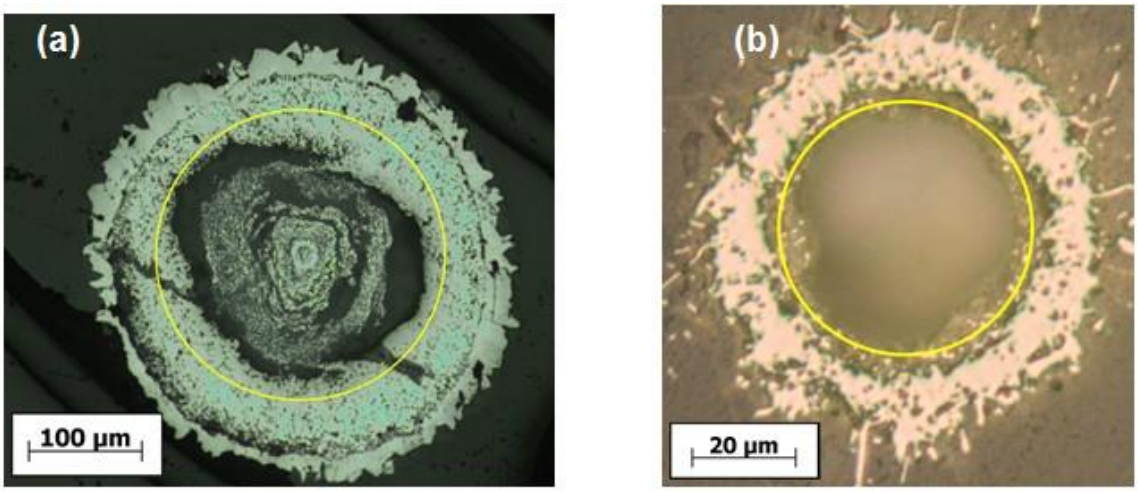

Figure 37: An optical micrograph of: (a) 250 µm wire oxidized at 1000 ºC for 20 hours. (b) 50 µm wire oxidized at 1000 ºC for 8 hours. A hollow core with oxides forming a tube-like structure can be observed in both the images.

CHAPTER FIVE: DISCUSSION

5.1 Oxidation Kinetics of Titanium Wire

5.1.1 Calculation of Reaction Rate Constants for Oxidation in Ar-20% O_2

By applying a kinetic model for cylindrical geometry on the available data of core diameter measurements, calculations of reaction rate constants were carried out. Kinetic models for cylindrical solids were derived (detailed derivation in the Appendix B section) using a similar approach to that used in the Jander's model for kinetics of solid-state reactions [41].

The plots for oxidation of different diameter Ti wires at 1000°C for linear, parabolic, and cubic kinetics are shown in Figures 38, 39, and 40, respectively.

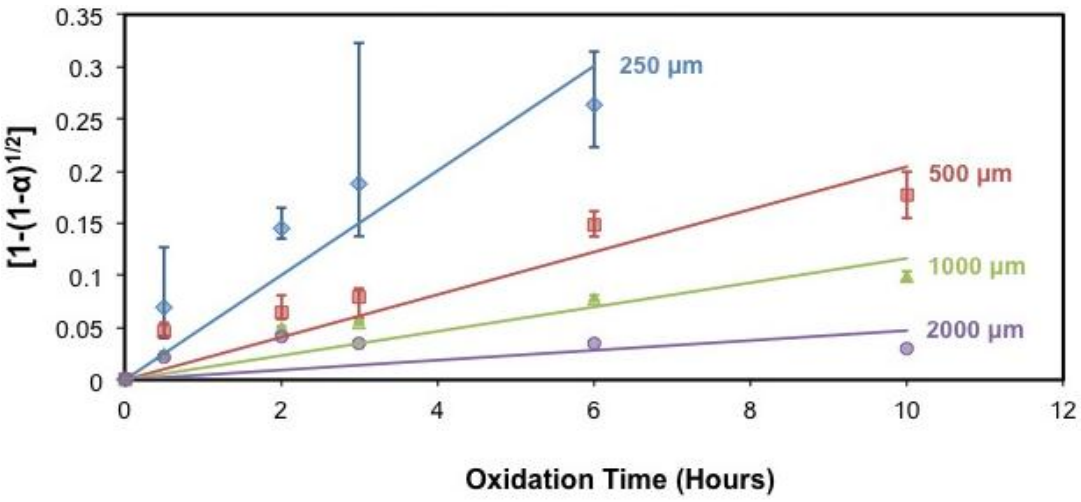

Figure 38: A plot for linear kinetics model derived using Jander's approach [41] for sample oxidized at 1000°C. The term α used in the plot is the fraction of reacted volume given by $\alpha = 1 - \left(\frac{r^2}{R^2}\right)$ where *R* and *r* is the radius of the Ti wire before and after oxidation, respectively.

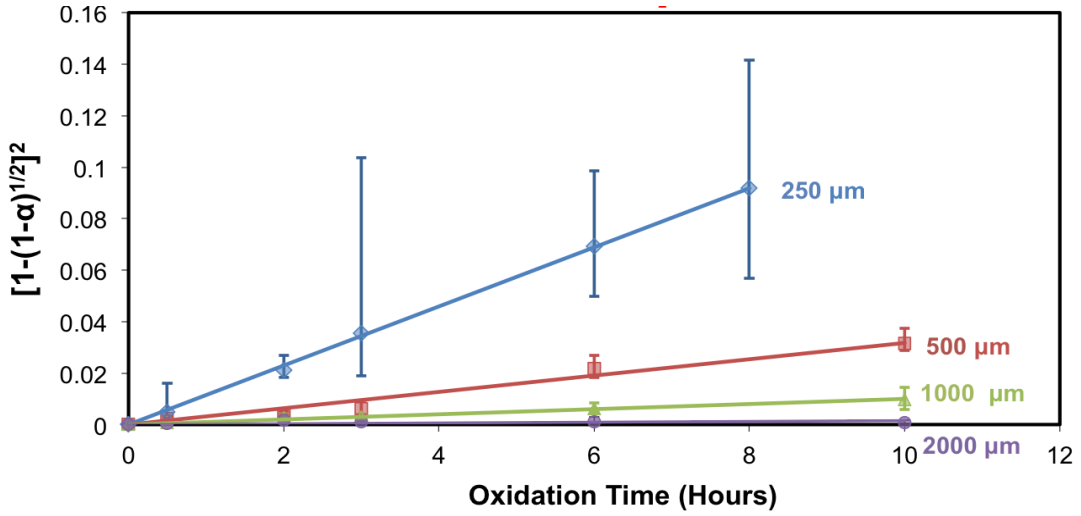

Figure 39: A plot for parabolic kinetics model derived using Jander's approach for sample oxidized at 1000°C.

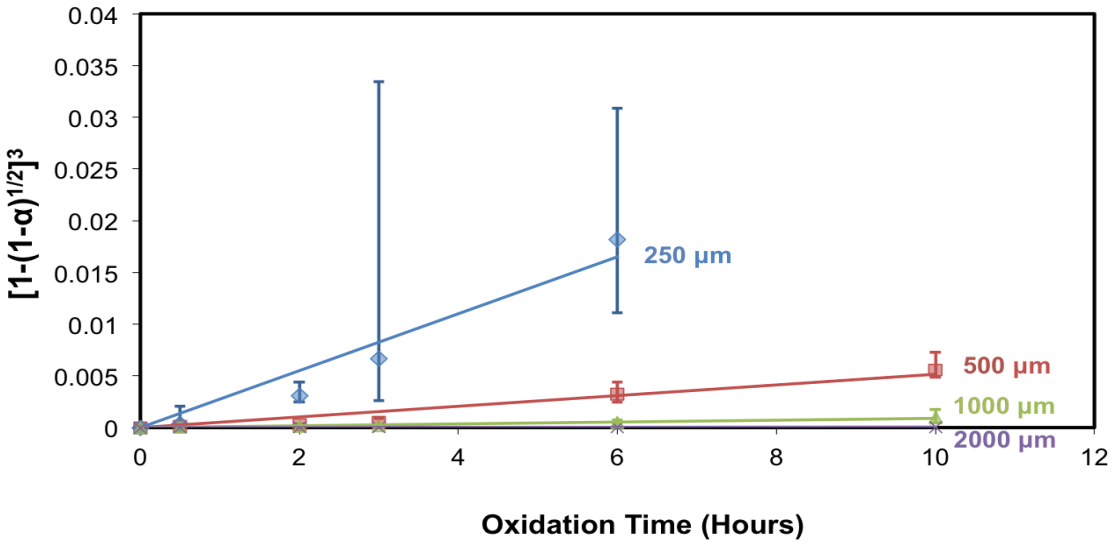

Figure 40: A plot for cubic kinetics model derived using Jander's approach for sample oxidized at 1000°C.

It was determined that the parabolic kinetics model provided with the best fit for the experimental data for oxidation at 1000°C (as can be observed by comparing Figures 37, 38, and 39). It is also important to note that only the data-points up to 10 hours of oxidation were considered after careful scrutiny of fitting the model. The data for oxidation beyond 10 hours of oxidation did not provide a good fit for either of the linear, parabolic, or cubic kinetics models, suggesting the oxidation kinetics might be a combination of parabolic and linear or para-linear as suggested by previous investigators [5, 10].

What can be inferred from this analysis is that the titanium wire oxidation at 1000°C closely follows parabolic kinetics in the initial stages of oxidation and further complex kinetics at higher oxidation times. As Kofstad suggested [34], the high temperature parabolic oxidation signifies that a thermal diffusion process is rate determining, which may include uniform diffusion of one or both of the reactants through

a growing compact scale, or a uniform diffusion of gas into the metal. Thus, the data suggested that the titanium wire oxidation at 1000°C is rate limited by either of following three processes:

1. Vacancy diffusion of oxygen ions through the oxide scale to undergo oxidation at the scale-metal interface.
2. Vacancy diffusion of Ti^{4+} ions through the oxide scale to undergo oxidation at the scale-gas interface.
3. Interstitial diffusion of O^{2-} ions into the Ti metal core.

Using a similar approach, linear, parabolic, and cubic kinetics models were also derived to fit the experimental data obtained for oxidation at 800 and 1200°C. The parabolic kinetics model provided a relatively better fit in all the cases. As mentioned in the background section, titanium oxidation proceeds with parabolic kinetics at initial stages and changes to a pseudo-linear kinetics after a certain interval of time and then finally changes to a 2^{nd} parabolic kinetics after prolonged oxidation. The closeness of the experimental data for oxidation at 800°C to the fit for the parabolic kinetics implies that the oxidation process might be still in the initial stages of oxidation up to 16 hours of oxidation. At 1200°C, however, the closeness of experiment data to the fit for parabolic kinetics model might be suggesting that the oxidation process proceeded with the 2^{nd} parabolic kinetics within a very short period of oxidation time.

The values of parabolic rate constants for different diameter wires used at 800, 1000, and 1200°C were calculated using the slope of the plots for the parabolic kinetics model. The values of the calculated parabolic rate constants are reported in Table 2.

Table 2: The calculated values of parabolic rate constants based on core diameter measurements for oxidation in Ar-20% O_2.

Sample size	**800°C** k_P (μm^2/sec)	**1000°C** k_P (μm^2/sec)	**1200°C** k_P (μm^2/sec)
50 μm	0.006	-	-
127 μm	0.00032	-	-
250 μm	0.00046	0.025	0.353
500 μm	0.00017	0.028	0.852
1000 μm	0.00171	0.034	1.252
2000 μm	0.00416	0.027	1.373

A few points noted from the calculated values of parabolic rate constants for oxidation in Ar-20% O_2 as reported in Table 2 are as follows:

1. The parabolic rate constant value increases as the temperature of oxidation increases for each sample size suggesting that the higher the temperature the faster the oxidation process.
2. Besides a few eccentricities, the k_P values tend to increase with increasing sample size. This might be because of more availability of Ti metal for oxidation and hence more possibility of oxygen dissolution in larger diameter wires.

5.1.2 Calculation of Apparent Activation Energy for Titanium Wire Oxidation

Even though the oxide scale morphology was found to be complex, the k_P values calculated were utilized in calculating the values of the apparent activation energy of the

overall oxidation process by preparing an Arrhenius plot of ln (k_P) vs. 1/T as shown in Figure 41.

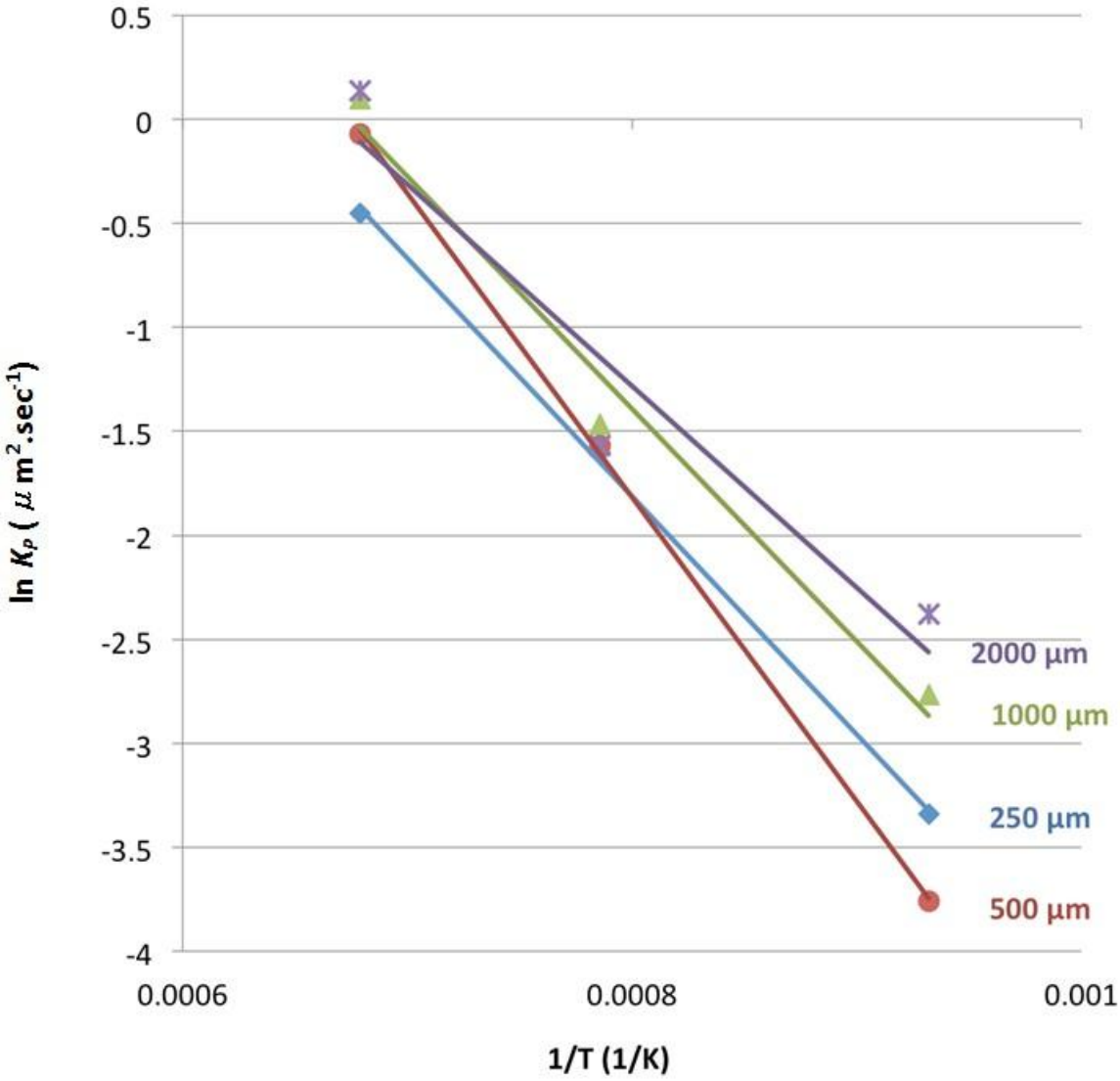

Figure 41: Arrhenius plot prepared using the parabolic rate constants calculated earlier. Slope of this plot provides activation energy for oxidation for each sample used.

The calculated values of the apparent activation energies for the overall oxidation of all the samples are reported in Table 3 along with the values of the activation energies reported by previous investigators on high temperature oxidation of bulk titanium.

Table 3: Apparent Activation Energy of oxidation of various sample sizes used in present work along with their comparison with activation energies reported in the literature.

	Specimen size	Oxidizing Conditions	Activation Energy (E_A) kJ/mol
Present Work	250 μm diameter wire	800 – 1200°C in Ar-20% O_2 at ~ 0.9 atm.	220
	500 μm diameter wire		280
	1000 μm diameter wire		210
	2000 μm diameter wire		190
John Stringer [10]	5 x 0.6 x 0.05 cm	850- 1000°C O_2 at ~< 1 atm.	260 (Oxygen dissolution)
			110 (Oxide scale)
Park and Butt [25]	12.5 mm x 2.75 mm disks	800 – 1400°C Ar-20% O_2 at 0.765 atm.	230
Jenkins *et al.*[7]	1.75 x 1.5 x 0.2 cm	600- 925°C in O_2 at ~ 0.92 atm.	250
Kofstad *et al.* [5]	1 x 1.5 x 0.2	800 – 1200°C O_2 at 1 atm.	250

The Arrhenius plot obtained for different sample sizes used in the present study shows that the slope of the line increases as the size of the sample decreases with the exception of the 250 μm diameter wire samples, for which, there were limited data points at higher temperatures due to their complete oxidation within a very short span of time.

By comparing the values of apparent activation energies calculated in this work to the values of activation energies reported by previous investigators (for oxidation in bulk Ti) as shown in Table 3, the following observations can be made:

1. Under similar oxidizing conditions, the apparent activation energies for the oxidation of Ti wires, which range from 190 to 280 kJ/mol agree closely with activation energies reported by the previous investigators for parabolic oxygen dissolution in bulk titanium as ranging from 230-260 kJ/mol. This suggests that the oxygen dissolution in the Ti metal core might be a rate limiting mechanism during oxidation of Ti wires at higher temperatures.
2. Since the apparent activation energy usually showed a decrease with an increase in size of samples, it could be inferred that the smaller Ti wire get much readily oxidized than larger wires due to faster complete saturation of Ti core with oxygen.

5.2 Comparison of Oxidation Behavior in Ar-20% O_2 and N_2-20% O_2

5.2.1 Comparison of the Rate Constants in Ar-20% O_2 and N_2-20% O_2

The values of residual core diameter from oxidation in N_2-20% O_2 at 1000°C were used to fit in Jander-like kinetic model as done earlier for wires oxidized in Ar-20%

O_2. The plot for parabolic kinetics was the best fit for the data, which is shown in Figure 42.

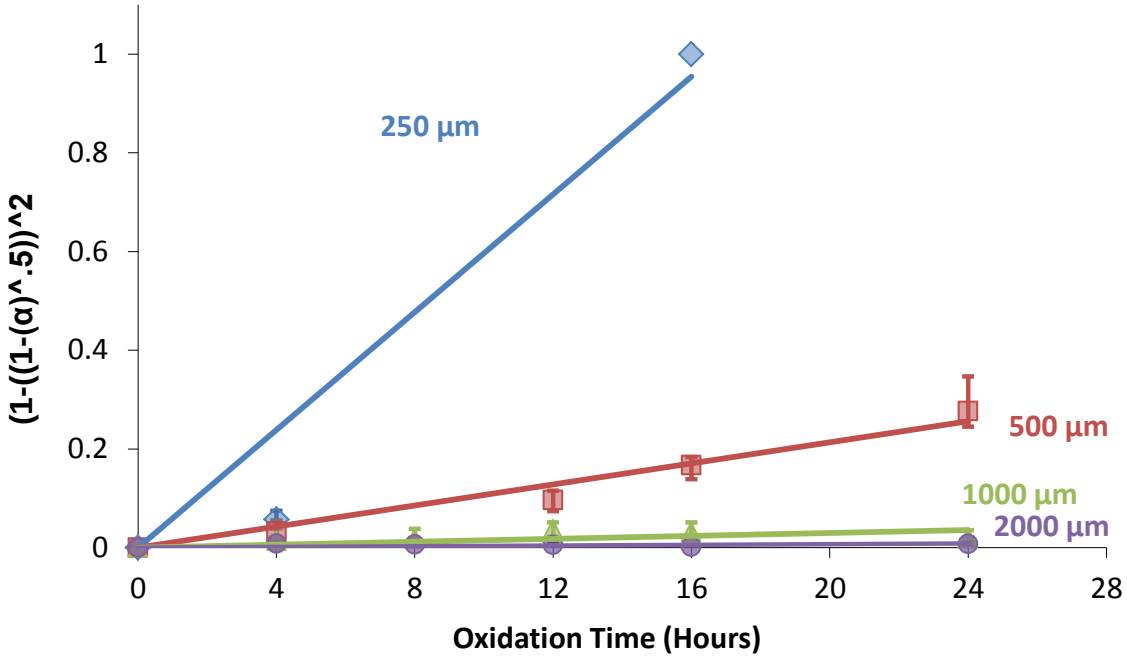

Figure 42: A plot for parabolic kinetics model derived using Jander's approach for sample oxidized at 1000°C in N_2-20% O_2.

The parabolic rate constants as calculated from the slope of the above plot for oxidation in N_2-20% O_2 along with those calculated earlier in Ar-20% O_2 are reported in Table 4.

Table 4: The values of parabolic rate constants for samples as calculated using the core diameter measurements from the parabolic kinetics models for oxidation in Ar-20% O_2 and N_2-20% O_2 at 1000°C.

Wire diameter	Ar-20% O_2at 1000°C (μm^2/sec)	N_2-20% O_2 at 1000°C (μm^2/sec)
250 µm	0.025	0.136
500 µm	0.027	0.093
1000 µm	0.034	0.051
2000 µm	0.027	0.041

The k_P values obtained show that the values were higher by about 2 to 5 times in N_2-20% O_2. It is important to note here that the reaction rate constants were obtained from core diameter measurements, which may vary in the two environments depending the extent of oxygen (and/or nitrogen) dissolution in the metal core. The outer oxide, measurements were found to be almost similar in the two environments because it was found to largely constitute the TiO_2 phase in both the cases.

5.2.2 Comparison of the TEM Characterization Results

It is important to note from Figure 15 that the TEM analysis of the 500 µm diameter sample oxidized at 1000°C for 8 hours in Ar-20% O_2 revealed that in all samples the outer-most oxide was found to be TiO_2 (rutile) and a there was a presence of a Ti_2O phase in the region next to the extremity of the residual metal core. However, in Figure 20, the results of the TEM analysis of the 500 µm diameter sample oxidized under identical conditions in N_2-20% O_2 showed that along with those phases determined in

sample oxidized in Ar-20% O2, there is a presence of a titanium nitride (TiN)/ nitrogen rich layer just above the residual metal core, which was followed by a region of Ti_2O above it.

Thus, the formation of this nitride layer might be the reason for differences in the measurements of oxide thickness, core diameter, and reaction rate constants for the samples oxidized in these two mediums. However, the data in the present work did not suggest that the oxidation rate in N_2-20% O_2 is lower than that in Ar-20% O_2 as proposed by previous studies [23, 40], but the rate was rather a little higher. The reasons for these differences might be the small size of the sample, the cylindrical geometry and/or a relatively shorter oxidation time than that used in previous investigations.

In another study of oxidation of bulk titanium at 800°C for 150 hours in nitrogen containing atmosphere by Gobel *et al.* [38], the dissolution of nitrogen in titanium was found to be significantly lower than the dissolution of oxygen and suggested only a slight decrease in oxidation rate than that in pure oxygen atmosphere. It is important to mention that the present work focused on collecting data and calculating reaction rates from the optical images on the samples. The measurement of only the apparent residual titanium, which might be saturated with oxygen and/or nitrogen during oxidation, was considered. Thus, higher oxygen dissolution in the metal might contribute to a higher oxidation rate in Ar-20% O_2 than that in N_2-20% O_2, as suggested in the literature [23, 38, 40].

5.3 Overall Interpretation of the Titanium wire Oxidation

5.3.1 Effects of Oxidation Temperature and Time

Morphological Changes

In the present work for oxidation in the temperature range from 800°C to 1200°C, the general effect of increasing the temperature of oxidation was that the samples underwent the various stages of morphological evolution within a shorter span of time. However, there were also certain specific morphological changes observed at different oxidation temperatures.

Observation of the morphological evolution at 800°C revealed that there were no distinctly visible regions in the core and oxide scale was porous and consisted of few layers of oxides. However, at 1000°C, the oxide scale was observed to possess multi-layers during the initial stages and a distinct compact outer oxide and porous inner oxide region at later stages. The primary reason is attributed to extensive dissolution of oxygen in the metal core at 1000°C owing to the dissolution of oxygen in β-Ti phase, conversion of β-Ti to α-Ti due to oxygen being α stabilizer, and subsequent dissolution of oxygen in α-Ti phase as cited in the literature [6, 10]. Prolonged oxidation of titanium wires resulted in sintering and grain growth of oxide scale and formation of a highly compact outer oxide scale of rutile and porous inner core. At 1200°C, as an exception, the presence of distinct layers of oxide was observed upon extended oxidation in some samples.

Changes in the Reaction Kinetics

As mentioned in the Results section, with increasing temperature of oxidation, the values of the parabolic rate constants, k_P (as obtained from the Jander-like kinetic model), increased for similar sample sizes.

As mentioned in the literature, the kinetic regime changes from an initial parabolic to linear and finally to a 2nd parabolic [10]. And on increasing the temperature, the span of changes in the kinetic regime gets shorter.

It was also worth noting that prolonged oxidation at any temperature of interest resulted in a complete dissolution of the core and the eventual formation of hollow tube-like structures with compact outer scales, inferring a probable outward diffusion of oxygen saturated Ti from the core.

5.3.2 Effect of Sample Size

The effect of decreasing the initial size of the sample, that is wire diameter, was somewhat similar to the effect of increasing the temperature of oxidation. Thus, the smaller the wire diameter, the faster it will proceed through various stages of morphological evolution and also shorter are the spans of each kinetic regime. This is because the smaller the initial diameter of the wire, the smaller is the interfacial area available for oxidation. Hence, smaller wires underwent oxidation faster under identical conditions. Again, as oxidation proceeds further, the residual wire radius kept decreasing and so did the available interfacial area for oxidation. For example, as shown in Figure 33, a 250 μm diameter titanium wire undergoes a relatively equal extent of oxidation in 6 hours at 1000°C as does a 500 μm diameter wire in 24 hours at the same temperature.

Hence, for the oxidation of wires or other cylindrical or spherical components, changes in the initial samples sizes might result in the extent of oxidation being 4-5 times faster.

5.3.3 Effect of Oxidizing Environment

The oxidation kinetics studies in Ar-20% O_2 and N_2-20% O_2 suggested that the oxidation rates are fairly close in the two environments at 1000°C. This observation is in disagreement with observations by Hanrahan and Butt [23] and Chen and Rosa [40] who reported that the oxidation rates in air and N_2-20% O_2 were significantly lower than those in Ar-20% O_2 due to the formation of a nitride layer (which was also detected in the present work). Measuring the apparent core diameter of the samples before and after oxidation was the basis of determining the reaction kinetics in the present work. However, work by Hanrahan and Butt, and Chen and Rosa involved a determination of reaction kinetics using thermo-gravimetric analysis. This shows that the method of measuring reaction kinetics can affect the determination of reaction rate when comparing changes due to the use of different oxidizing medium. It also confirms that the mechanism of titanium wire oxidation is complex with overlapping kinetics and conclusions of the rate limiting mechanism cannot be deduced with certainty even when many different approaches are considered.

5.3.4 Complex Nature of the Oxide Scale and Competing Reaction Kinetics

The complex nature of the oxide scale morphology and wide scatter and the ambiguity in the kinetics data as observed in the present study, makes us believe that the oxidation mechanism of titanium wire in the temperature range of 800-1200°C is indeed quite complex involving competing reactions as cited by numerous authors in the

literature for the oxidation mechanism of bulk titanium [6, 7, 10, 18, 24, 25]. Even though the data in the present study showed a good fit for parabolic kinetics and calculations of activation energy for titanium wire samples generally showed good agreement with activation energy for oxygen dissolution in the metal core, it is important to note that the kinetic model used in the present study is quite simple in nature compared to the complicated oxidation mechanism prevalent. There are numerous factors to be considered to further refine the kinetics model for the present study like:

- Volume expansion of the oxide scale,
- Porosity of the oxide scale,
- Constantly changing scale-metal interfacial area,
- Moving scale-metal and scale-gas interface boundaries, and
- Dissolution of oxygen in the metal core.

CHAPTER SIX: CONCLUSIONS

The thermal oxidation kinetics of titanium wire of varying diameters between 50 and 2000 μm was assessed in Ar-20% O_2 in the temperature range 800-1200°C and in N_2-20% O_2 at 1000°C. Based on measurements of oxide thickness, optical and electron microscopy, and fitting the data to a shrinking core model for a cylindrical geometry, the following conclusions were reached:

1. In all wire samples, there was observed both the simultaneous formation of a multi-phase oxide comprised of at least TiO_2 and Ti_2O, and the dissolution of oxygen in the base Ti metal.
2. The morphological evolution of the oxide scale was documented at 1000°C as a function of diameter for times up to 24 hours. The oxide grows outward due to the rapid diffusion of Ti and, due to the volume difference between the oxide and the base metal, the oxide separates from the metal forming a lamellar oxide structure. At long times, the layers sinter together and there is significant grain growth in the outer oxide, the oxide grows away from the shrinking metal core leading to the development of a gap between the outer oxide scale and the residual metal.
3. Using the data from measured core diameters, a shrinking core model was adapted from Jander [41] and used to obtain a best fit to experimental results. From the fits to the model, estimates of parabolic rate constants were obtained. These values were used to obtain apparent activation energies, which were compared to reported values in the literature for oxidation of Ti and pertinent diffusivities. The apparent activation

energies varied from 190 to 280 kJ/mol. Key references in the literature [5, 7, 10, 24] for the oxidation of monolithic Ti indicate that the activation energy for oxidation (as evaluated through the parabolic rate constant) is in the range 220 to 250 kJ/mol. Consequently, this study is not inconsistent with those previous studies that were based on weight loss measurements rather than these measurements of core diameters. Based on these comparisons with prior studies and the analyses of the oxidation mechanisms of Stringer [10] , and Hanrahan and Butt [24] it is suggested that the oxidation of the Ti wires investigated here was rate limited by dissolution of oxygen in Ti metal core.

4. Present work also constitutes comparison of oxidation behavior of titanium wires in Ar-20% O_2 and N_2-20% O_2. The study showed that the oxidation rate in the two environments closely relate to each other with oxidation rate in N_2-20% O_2 being slightly higher. Previous work [23, 40] has demonstrated that the oxidation of Ti in air or nitrogen containing gas is inhibited by the formation of the TiN layer. In these studies, a TiN layer was also observed by TEM. However, there was no strong evidence in the present work that suggested that the TiN layer inhibited the oxidation process.
5. Under optimized conditions, rutile micro-tubes were produced. While the parameter space was exhaustively investigated, using the smaller diameter wire hollow rutile tubes were produced during oxidation at 1000°C and 8 hours, and 800°C and 16 hours.

REFERENCES

[1] M.J. Donachie, Titanium and titanium alloys, American Society for Metals, Metals Park, Ohio, 1982.

[2] K.O. Awitor, S. Rafqah, G. Geranton, Y. Sibaud, P.R. Larson, R.S.P. Bokalawela, J.D. Jernigen, M.B. Johnson, "Photo-catalysis using titanium dioxide nanotube layers", *Journal of Photochemistry and Photobiology a-Chemistry*, vol. 199, pp. 250-254, 2008.

[3] J.S. Dalton, P.A. Janes, N.G. Jones, J.A. Nicholson, K.R. Hallam, G.C. Allen, "Photocatalytic oxidation of NO_x gases using TiO_2: A surface spectroscopic approach", *Environmental Pollution*, vol. 120, pp. 415-422, 2002.

[4] P. Kofstad, "High-temperature oxidation of titanium", *Journal of the Less-Common Metals*, vol. 12, pp. 449-464, 1967.

[5] P. Kofstad, P.B. Anderson, O.J. Krudtaa, "Oxidation of titanium in the temperature range 800-1200 degrees C", *Journal of the Less-Common Metals*, vol. 3, pp. 89-97, 1961.

[6] P. Kofstad, K. Hauffe, H. Kjollesdal, "Investigation on the oxidation mechanism of titanium", *Acta Chemica Scandinavica*, vol. 12, pp. 239-266, 1958.

[7] A.E. Jenkins, "The oxidation of titanium at high temperatures in an atmosphere of pure oxygen", *Journal of the Institute of Metals*, vol. 82, pp. 213-221, 1954.

[8] A.E. Jenkins, "A further study of the oxidation of titanium and its alloys at high temperatures", *Journal of the Institute of Metals*, vol. 84, pp. 1-9, 1955.

[9] G.R. Wallwork, A.E. Jenkins, "Oxidation of titanium, zirconium, and hafnium", *Journal of the Electrochemical Society*, vol. 106, pp. 10-14, 1959.

[10] J. Stringer, "The oxidation of titanium in oxygen at high temperatures", *Acta Metallurgica*, vol. 8, pp. 758-766, 1960.

[11] J. Stringer, "The effect of pressure on the 2nd stage parabolic rate in the oxidation of titanium", *Acta Metallurgica*, vol. 8, pp. 810-811, 1960.

[12] J. Stringer, "Some observations on the kinetics of oxidation of titanium at high temperatures", *Journal of the Less-Common Metals*, vol. 6, pp. 207-213, 1964.

[13] M.H. Davies, C.E. Birchenall, "Oxidation of titanium", *Journal of Metals*, vol. 3, pp. 877-880, 1951.

[14] P.H. Morton, W.M. Baldwin, "The scaling of titanium in air", *Transactions of the American Society for Metals*, vol. 44, pp. 1004-1029, 1952.

[15] S. Andersson, B. Collen, G. Kruuse, U. Kuylenstierna, A. Magneli, H. Pestmalis, S. Asbrink, "Identification of titanium oxides by X-ray powder patterns", *Acta Chemica Scandinavica*, vol. 11, pp. 1653-1657, 1957.

[16] S. Andersson, B. Collen, U. Kuylenstierna, A. Magneli, "Phase analysis studies on the titanium-oxygen system", *Acta Chemica Scandinavica*, vol. 11, pp. 1641-1652, 1957.

[17] J.E. Lopes Gomes, A.M. Huntz, "Correlation between the oxidation mechanism of titanium under a pure oxygen atmosphere, morphology of the oxide scale, and diffusional phenomena", *Oxidation of Metals*, vol. 14, pp. 249-261, 1980.

[18] J. Unnam, R.K. Clark, "Oxidation of commercial purity titanium", *Oxidation of Metals*, vol. 26, pp. 231-252, 1986.

[19] G. Bertrand, K. Jarraya, J.M. Chaix, "Morphology of oxide scales formed on titanium", *Oxidation of Metals*, vol. 21, pp. 1-19, 1984.

[20] T. Hurlen, "Oxidation of titanium", *Journal of the Institute of Metals*, vol. 89, pp. 128-136, 1960.

[21] P.B. Entchev, D.C. Lagoudas, J.C. Slattery, "Effects of non-planar geometries and volumetric expansion in the modeling of oxidation in titanium", *International Journal of Engineering Science*, vol. 39, pp. 695-714, 2001.

[22] P.K. Imbrie, D.C. Lagoudas, "Morphological evolution of TiO_2 scale formed on various 1D and 2D geometries of titanium", *Oxidation of Metals*, vol. 55, pp. 359-399, 2001.

[23] R.J. Hanrahan, D.P. Butt, "The effects of nitrogen on the kinetics and mechanisms of oxidation of titanium-tantalum alloys", *Oxidation of Metals*, vol. 48, pp. 41-58, 1997.

[24] R.J. Hanrahan, D.P. Butt, "Oxidation kinetics and mechanisms of ti-ta alloys", *Oxidation of Metals*, vol. 47, pp. 317-353, 1997.

[25] Y. Park, D.P. Butt, "Composition dependence of the kinetics and mechanisms of thermal oxidation of titanium-tantalum alloys", *Oxidation of Metals*, vol. 51, pp. 383-402, 1999.

[26] E.A. Gulbransen, K.F. Andrew, "Kinetics of the reactions of titanium with O_2, N_2 and H_2", *Transactions of the American Institute of Mining and Metallurgical Engineers*, vol. 185, pp. 741-748, 1949.

[27] E.-S. Oh, "Kinetics and kinematics for the metal oxidation on a spherical geometry", *Chemical Engineering Journal*, vol. 135, pp. 157-167, 2008.

[28] Y.T. Zhu, S.T. Taylor, M.G. Stout, D.P. Butt, T.C. Lowe, "Kinetics of thermal, passive oxidation of nicalon fibers", *Journal of the American Ceramic Society*, vol. 81, pp. 655-660, 1998.

[29] D.P. Butt, "Private conversation", 2008.

[30] J. Murray, H. Wriedt, "The O−Ti (oxygen-titanium) system", *Journal of Phase Equilibria*, vol. 8, pp. 148-165, 1987.

[31] P.G. Wahlbeck, P.W. Gilles, "Reinvestigation of phase diagram for system titanium-oxygen", *Journal of the American Ceramic Society*, vol. 49, pp. 180-184, 1966.

[32] T. Smith, "Oxidation of titanium between 25 degrees C and 400 degrees C", *Surface Science*, vol. 38, pp. 292-312, 1973.

[33] W.A. Alexander, L.M. Pidgeon, "Kinetics of the oxidation of titanium", *Canadian Journal of Research Section B-Chemical Sciences*, vol. 28, pp. 60-72, 1950.

[34] P. Kofstad, "High temperature corrosion", Elsevier Applied Science, New York, NY, USA, 1988.

[35] P. Kofstad, "High-temperature oxidation of metals", Wiley, New York, 1966.

[36] N. Birks, G.H. Meier, F.S. Pettit, Introduction to the high-temperature oxidation of metals, Cambridge University Press, Cambridge, UK, 2006.

[37] D.C. Lagoudas, P. Entchev, R. Triharjanto, "Modeling of oxidation and its effect on crack growth in titanium alloys", *Computer Methods in Applied Mechanics and Engineering*, vol. 183, pp. 35-50, 2000.

[38] M. Gobel, J.D. Sunderkotter, D.I. Mircea, H. Jenett, M.F. Stroosnijder, "Study of the high-temperature oxidation behaviour of Ti and Ti-4Nb with SNMS using tracers", *Surface and Interface Analysis*, vol. 29, pp. 321-324, 2000.

[39] P. Perez, "On the influence of water vapour on the oxidation behaviour of pure Ti", *Corrosion Science*, vol. 49, pp. 1172-1185, 2007.

[40] Y.S. Chen, C.J. Rosa, "Oxidation characteristics of Ti-4.37 wt. % Ta alloy in the temperature range 1258-1473 K", *Oxidation of Metals*, vol. 14, pp. 167-185, 1980.

[41] W. Jander, "Reactions in solid states at room temperature: I. Announcement: The rate of reaction in endothermic conversions", *Z. Anorg. Allg. Chem.*, vol. 163, pp. 1-30, 1927.

[42] R.E. Carter, "Kinetic model for solid-state reactions", *Journal of Chemical Physics*, vol. 34, pp. 2010-2015, 1961.

[43] H.G. Jiang, Y.T. Zhu, D.P. Butt, "Oxidation kinetics of hexagonal-shaped single-crystal silicon whiskers", *Journal of the American Ceramic Society*, vol. 82, pp. 2791-2795, 1999.

[44] G.S. Rohrer, Structure and bonding in crystalline materials, Cambridge University Press, Cambridge; New York, 2001.

[45] E. Sanchez, T. Lopez, R. Gomez, Bokhimi, A. Morales, O. Novaro, "Synthesis and characterization of sol-gel Pt/TiO_2 catalyst", *Journal of Solid State Chemistry*, vol. 122, pp. 309-314, 1996.

APPENDIX A

Measurement of Outer Oxide Thickness in Ar-20% O_2

APPENDIX A

Measurement of Outer Oxide Thickness in Ar-20% O_2

The cross-section of a 500 μm wire oxidized at 1200°C for 3 hours in below showed different regions of oxides. It was observed that many oxidized samples possessed a distinct, compact outer oxide layer at higher oxidation temperature and dwell time. The XRD, XPS, and TEM analysis suggested that this outer oxide layer is essentially TiO_2 (rutile). Thus, the thickness of this distinct outer layer was measured for all the oxidized samples and the thickness measurements were represented as a function of time.

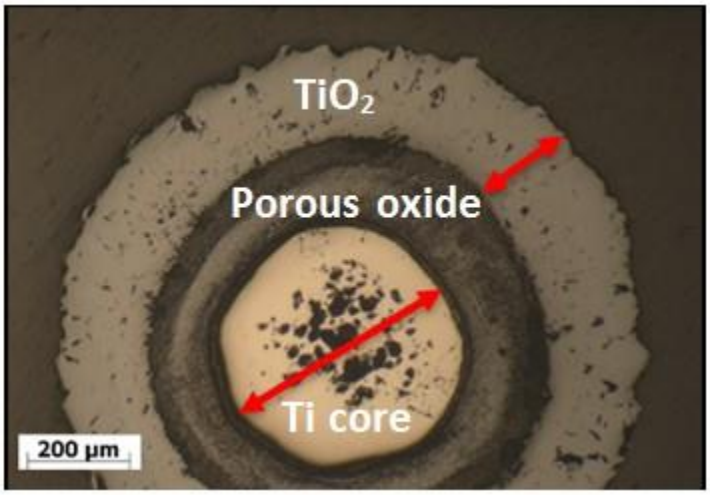

Figure 43: An optical micrograph of a 500 μm wire oxidized at 1200°C for 3 hours showing different layers of oxides in the sample. The arrows indicate the areas that were measured, that is, core diameter and outer-most oxide thickness.

A plot of outer oxide thickness versus time for all the samples exposed to Ar-20% O_2 at 800°C is shown in Figure 44. Each data point in the plot represents an average value of 6-10 measurements of oxide thickness over a single cross-section of the specific

diameter wire concerned. Each error bar represents the highest and the lowest value of oxide thickness measured.

The oxide thickness versus time plot for oxidation at 1000°C in Ar-20% O_2 for different size samples is shown in Figure 45. In this plot, the data points were obtained by measuring 4-6 different cross-sections of oxidized titanium wires. Each data point denotes a cumulative average of oxide thickness measured from different cross-sections. Each error bar represents the highest and the lowest value of oxide thickness measured from 4-6 different cross-sections.

The data for oxidation at 1200°C in Ar-20% O_2 was obtained in a similar way as that for oxidation at 800°C. The oxide thickness versus time plots for oxidation at 1000°C in Ar-20% O_2 for smaller and larger diameter wires are shown in Figure 46 and Figure 47, respectively.

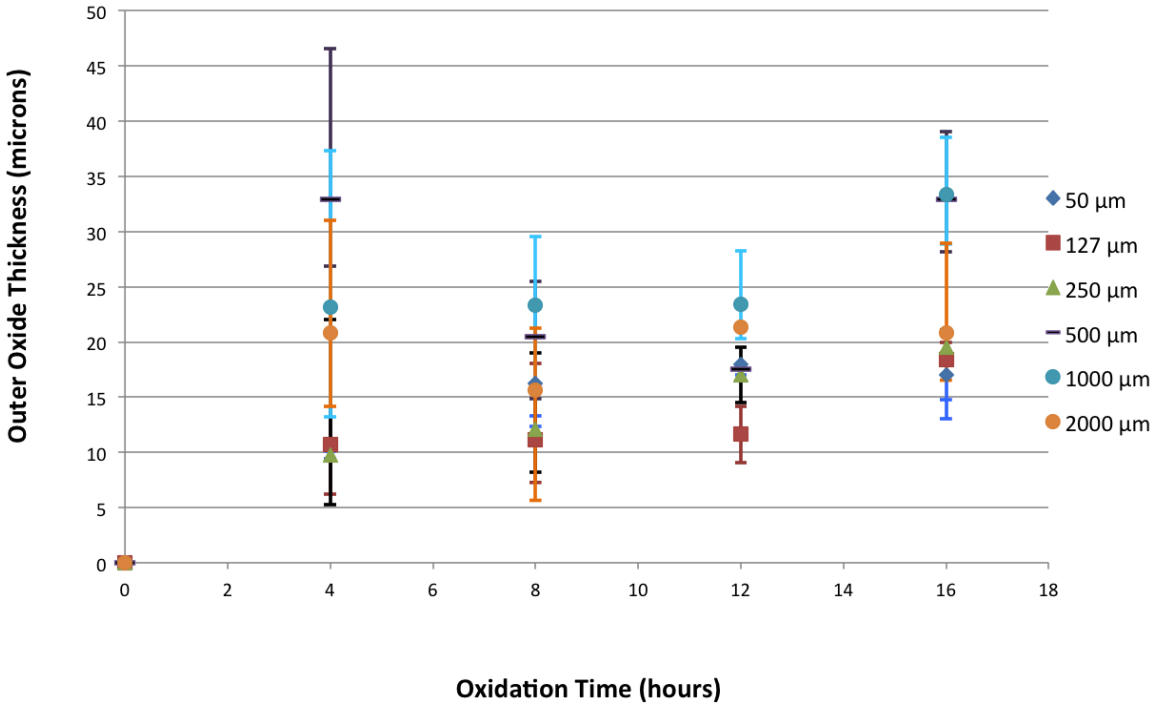

Figure 44: A plot of outer oxide thickness vs. time for samples exposed to Ar-20% O_2 at 800°C.

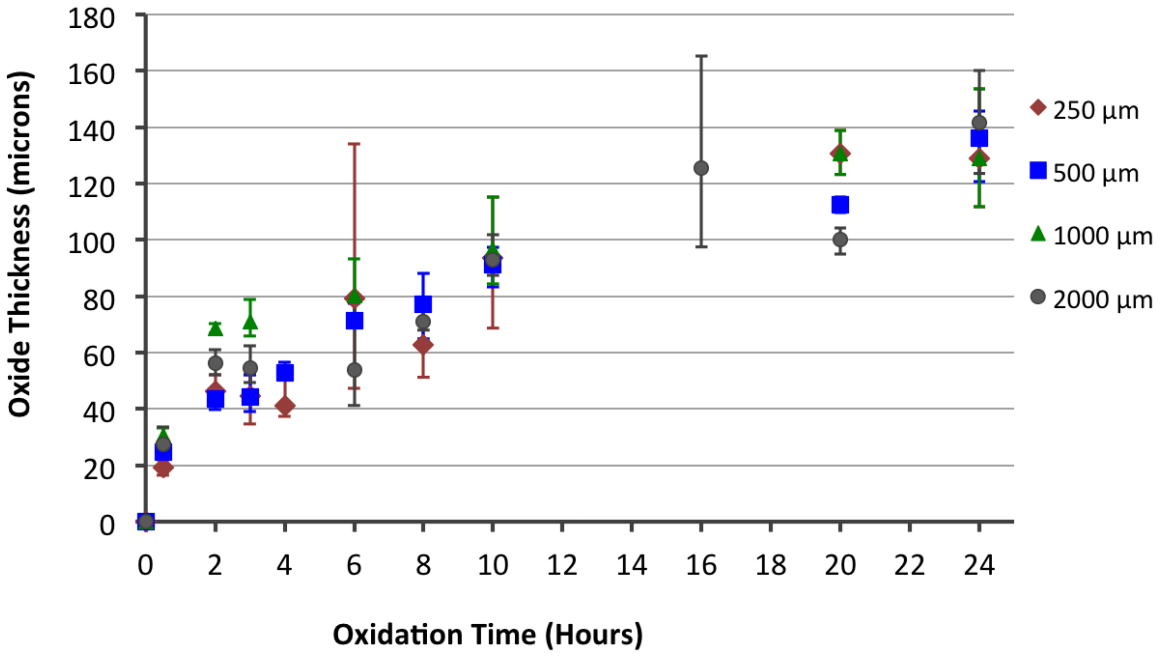

Figure 45: A plot of outer oxide thickness vs. time for samples exposed to Ar-20% O_2 at 1000°C.

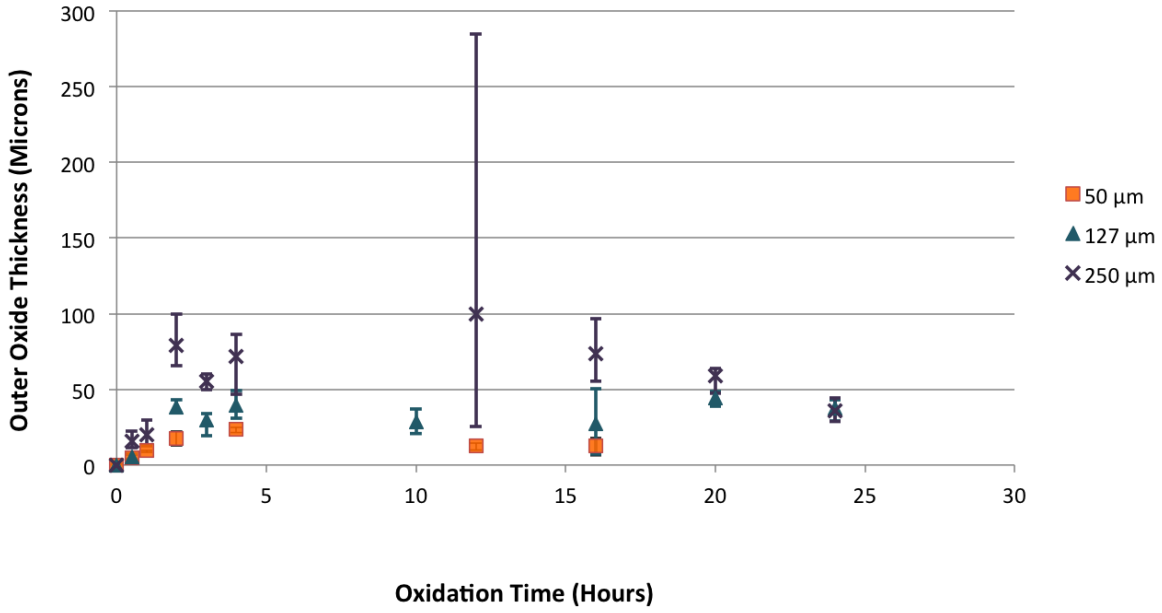

Figure 46: A plot of outer oxide thickness vs. time for samples exposed to Ar-20% O_2 at 1200°C.

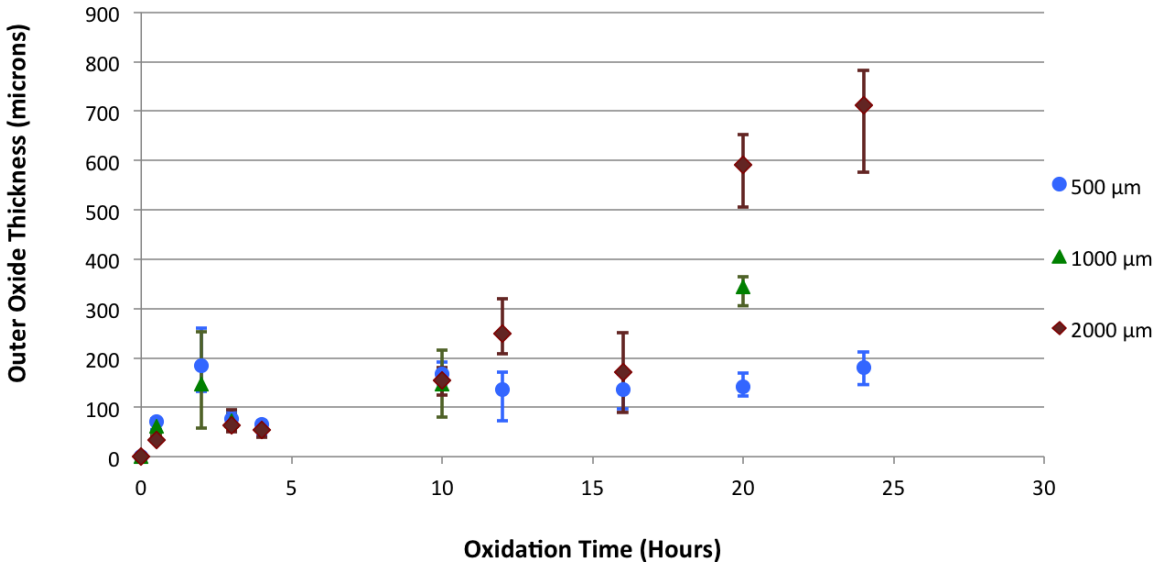

Figure 47: A plot of outer oxide thickness vs. time for samples exposed to Ar-20% O_2 at 1200°C.

It can be observed from Figures 44 to 47, both the 800°C and 1200°C data showed a larger margin of error than that for 1000°C. This is because the data is obtained from only a single cross-section of a sample and not from multiple cross-sections of a sample or multiple samples, as in the case of 1000°C samples. Also, some samples had a preferential growth of the oxide scale in certain directions resulting in a thick layer on one side and a very thin layer on the other side. Shown in Figure 48 is an example of such an oxide growth.

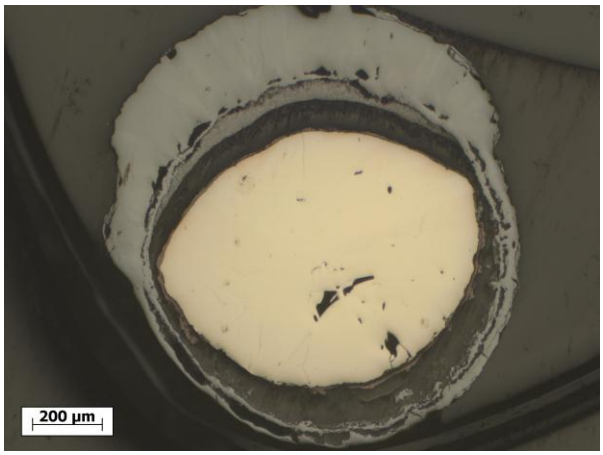

Figure 48: A micrograph of a 1000 µm Ti wire oxidized at 1200°C for 2 hours clearly presenting an example of the preferential oxidation of the metal in a certain region causing a scatter in the data measured.

APPENDIX B

Derivation of Jander-like Kinetics Model for Cylindrical Solids

APPENDIX B

Derivation of Jander-like Kinetics Model for Cylindrical Solids

A kinetics model for cylindrical solids was derived utilizing the concept similar to the Jander's approach, which is discussed in detail below.

The initial volume of a solid cylindrical wire is given by:

$$V = \pi R^2 L \tag{2}$$

where, *R* is the initial radius of the wire,

L is the length of the wire

However, since in the present work the length of the wires were far too large in comparison to the diameter of their cross-sections, the value of the length of the wires was considered constant (= infinity) with respect to their diameters.

If the complete surface of the cylindrical wire was reacting with a gaseous component and developing a reaction product (oxide) of thickness *x*, assuming that the reaction was diffusion limited and the product had a parabolic growth rate such that:

$$dx/dt = k_P/x \tag{3}$$

where, k_P is the parabolic rate constant which upon integration gives

$$x^2 = 2\, k_P t \tag{4}$$

Thus, the volume of the unreacted Ti wire after an exposure time *t* is given by:

$$V = \pi\, (R - x)^2\, L \tag{5}$$

Where, *x* = the thickness of the oxide product formed

Now, considering α is the fraction of reacted volume of the Ti wire after exposure time *t*, the fraction of unreacted Ti wire can also be represented by:

$$V = \pi R^2 (1 - \alpha) L \quad (6)$$

Now, on equating the above two equations (5) and (6), we get:

$$x = R (1 - \sqrt{1 - \alpha}) \quad (7)$$

The above-obtained value of oxide thickness *x* can be incorporated into the integrated form of parabolic relation from equation (4) to get:

$$[R (1 - \sqrt{1 - \alpha})]^2 = 2 k_P t \quad (8)$$

Rearranging the above equation (8) gives the Jander-like parabolic kinetics model for the cylindrical geometry in the form:

$$(1 - \sqrt{1 - \alpha})^2 = (2k_P/R^2) t \quad (9)$$

A plot of $[1 - \sqrt{(1 - \alpha)}]^2$ versus oxidation time *t* will give a straight line with a slope as $2k_P/R^2$.

Similarly, a Jander-like linear kinetics model for the cylindrical geometry can be represented by:

$$1 - \sqrt{1 - \alpha} = (2k_L/R) t \quad (10)$$

Similarly, a cubic kinetics model can be given by:

$$(1 - \sqrt{1 - \alpha})^3 = (2k_C/R^3) t \quad (11)$$

Thus, if we know the initial radius (or diameter) of the wire *R* and the residual core radius (or diameter) of the wire *r* after it underwent oxidation for time *t*, then we can deduce the value of α using the relation:

$$\alpha = \frac{\pi R^2 L - \pi r^2 L}{\pi R^2 L} \tag{12}$$

Where, since π and *L* are constant the equation reduces to the form:

$$\alpha = 1 - \left(\frac{r^2}{R^2}\right) \tag{13}$$

Hence, using specific values of α after oxidation for a specific time *t*, we can approximate whether the oxidation is governed by linear, parabolic, or cubic kinetics. For this reason, at a specific temperature, the residual core diameter values of different Ti wire samples for a specific oxidation time were measured and the values of α were calculated in the present work. The values of α were subsequently fit in the kinetics models for linear, parabolic, and cubic regimes and the best fit was considered the probable oxidation kinetics at that temperature.